

# 1 TRENDS AND VARIABILITY IN THE OCEAN CARBON SINK

2 *Nicolas Gruber<sup>1,†</sup>, Dorothee C. E. Bakker<sup>2</sup>, Tim DeVries<sup>3</sup>, Luke Gregor<sup>1</sup>, Judith Hauck<sup>4</sup>, Peter*  
 3 *Landschützer<sup>5,6</sup>, Galen A. McKinley<sup>7</sup>, Jens Daniel Müller<sup>1</sup>.*

- 4 **1) *Environmental Physics, Institute of Biogeochemistry and Pollutant Dynamics, ETH Zurich,***  
 5 ***Zürich, Switzerland.***
- 6 **2) *Centre for Ocean and Atmospheric Sciences, School of Environmental Sciences, University of***  
 7 ***East Anglia, Norwich, UK.***
- 8 **3) *Department of Geography and Earth Research Institute, University of California, Santa Barbara,***  
 9 ***CA, USA.***
- 10 **4) *Alfred-Wegener-Institut, Helmholtz-Zentrum für Polar und Meeresforschung, Bremerhaven,***  
 11 ***Germany.***
- 12 **5) *Max Planck Institute for Meteorology, Hamburg, Germany.***
- 13 **6) *Flanders Marine Institute (VLIZ), Ostend, Belgium***
- 14 **7) *Columbia University and Lamont Doherty Earth Observatory, Palisades, NY, USA.***

15  
 16 **†e-mail: [nicolas.gruber@env.ethz.ch](mailto:nicolas.gruber@env.ethz.ch)**

## 17 **Abstract**

18  
 19  
 20  
 21 The ocean has absorbed  $25 \pm 2\%$  of the total anthropogenic CO<sub>2</sub> emissions from early 1960s to the late 2010s,  
 22 with rates more than tripling over this period and with a mean uptake of  $-2.7 \pm 0.2$  Pg C yr<sup>-1</sup> for the period 1990  
 23 through 2019. This growth of the ocean sink matches expectations based on the increase in atmospheric CO<sub>2</sub>,  
 24 but research has shown that the sink is more variable than long assumed. In this Review, we discuss trends and  
 25 variations in the ocean carbon sink. The sink stagnated during the 1990s with rates hovering around  $-2$  Pg C yr<sup>-1</sup>  
 26 <sup>1</sup>, but strengthened again after  $\sim 2000$ ,  $-$ uptaking over  $-3$  Pg C yr<sup>-1</sup> for 2010-2019. The most conspicuous changes  
 27 in uptake occurred in the high latitudes, especially the Southern Ocean. These variations are caused by changes  
 28 in weather and climate, but a volcanic eruption-induced reduction in the atmospheric CO<sub>2</sub> growth rate and the  
 29 associated global cooling contributed as well. Understanding the variability of the ocean carbon sink is crucial  
 30 for policy making and projecting its future evolution, especially in the context of the UN Framework  
 31 Convention on Climate Change stocktaking activities and the deployment of carbon dioxide removal methods.  
 32 This goal will require a global-level effort to sustain and expand the current observational networks and to  
 33 better integrate these observations with models.

34  
 35

36 **Table of contents summary**

37 Carbon uptake by the ocean has increased alongside rising atmospheric CO<sub>2</sub> concentrations, but with substantial  
38 variability. This Review examines trends in ocean CO<sub>2</sub> uptake and the internal and external factors driving its  
39 variability, finding an ocean uptake rate of  $-2.7 \pm 0.2$  Pg C yr<sup>-1</sup> for the period 1990 through 2019.

40

41 **Key points**

42

43 i) The long-term trend in the ocean carbon sink since the early 1960s was primarily driven by the increasing  
44 uptake of anthropogenic CO<sub>2</sub>. Although the ocean is expected to have lost a few petagrams of natural CO<sub>2</sub>  
45 to the atmosphere in response to ocean warming, this loss cannot be quantified conclusively with  
46 observations.

47 ii) The oceanic uptake of anthropogenic CO<sub>2</sub> scaled proportionally with the increase in atmospheric CO<sub>2</sub>  
48 between the early 1960s and late 2010s, as expected given the quasi-exponential growth of atmospheric  
49 CO<sub>2</sub> during this period.

50 iii) The average ocean uptake rate of  $-2.7 \pm 0.2$  Pg C yr<sup>-1</sup> for the period 1990 through 2019 yields a  
51 proportionality  $\beta$  of  $1.4 \pm 0.1$  Pg C per ppm of atmospheric CO<sub>2</sub>, suggesting a trend in the uptake of -  
52  $0.4 \pm 0.1$  Pg C yr<sup>-1</sup> decade<sup>-1</sup>.

53 iv) The ocean carbon sink varies by about  $\pm 20\%$  around this trend, primarily caused by changes in the  
54 sources and sinks of natural CO<sub>2</sub>, with a lesser role for variations in atmospheric CO<sub>2</sub> growth rates  
55 impacting the uptake of anthropogenic CO<sub>2</sub>.

56 v) The net oceanic uptake rate of CO<sub>2</sub> will likely decrease in the future owing to several converging trends:  
57 reduced emissions of CO<sub>2</sub> leading to reduced atmospheric CO<sub>2</sub> growth rates in response to climate policy;  
58 reduced storage capacity owing to continuing ocean acidification; and enhanced outgassing of natural  
59 CO<sub>2</sub> owing to ocean warming and changes in ocean circulation and biology.

60

61

## 62 [H1] Introduction

63

64 Throughout the Anthropocene, the ocean has been the largest and most persistent sink for the anthropogenic  
65 CO<sub>2</sub> emitted into the atmosphere by the burning of fossil fuels, cement production, and land use change<sup>1-4</sup>.  
66 This importance was recognized already by the late 19<sup>th</sup> century<sup>5,6</sup>, with the chemist Arrhenius<sup>7</sup> estimating  
67 that about 83% of the emitted anthropogenic CO<sub>2</sub> would be taken up by the ocean. Therefore, he concluded  
68 that no noticeable global warming should be expected from the emissions of anthropogenic CO<sub>2</sub>, since the  
69 uptake by the ocean uptake leave only a small fraction of the emissions accumulating in the atmosphere.  
70 Although his estimate of the long-term capacity of ocean uptake was accurate<sup>8,9</sup>, Arrhenius was not aware  
71 that it takes thousands of years for the ocean to fully realize this capacity and not decades as he implicitly  
72 assumed<sup>6</sup>. Arrhenius' view was widely shared, so that the scientific community was oblivious to the growing  
73 threat from the CO<sub>2</sub> emissions that were increasing by several percent per year for most of the early 20<sup>th</sup>  
74 century<sup>10</sup>. Revelle and Suess<sup>11</sup> realized this mistake in 1957. Thereafter, the perspective of the scientific  
75 community on the issue of human-induced climate change shifted rapidly<sup>12,13</sup>, especially after Keeling  
76 confirmed in 1960 that atmospheric CO<sub>2</sub> was increasing much more rapidly than implied by Arrhenius<sup>14</sup>.

77 Much of global ocean carbon cycle research since Revelle and Suess' discovery has focused on quantifying  
78 the fraction of the CO<sub>2</sub> emissions taken up by the ocean, and to understand the processes that limit this  
79 uptake, preventing the ocean from reaching the huge capacity of more than 80% that Arrhenius had  
80 identified. A crucial step to address this question was the conceptualization of the net exchange of CO<sub>2</sub> across  
81 the air-sea interface and the change in the stock of **dissolved inorganic carbon (DIC) [G]** to consist of two  
82 components: anthropogenic CO<sub>2</sub> and natural CO<sub>2</sub> (Box 1). The anthropogenic CO<sub>2</sub> component, previously  
83 often referred to as excess CO<sub>2</sub><sup>15</sup>, can be considered the perturbation component, as it is solely a consequence  
84 of the anthropogenic increase in atmospheric CO<sub>2</sub>. The natural CO<sub>2</sub> component of the flux is associated with  
85 the pre-industrial pool of DIC in the ocean (order of 37,000 Pg C (1 Pg 10<sup>15</sup>g)<sup>16</sup> and is involved in **air-sea gas**  
86 **exchange [G]**, uptake and release by the biological pumps, interactions with and loss to the sediments, and  
87 input by rivers (Box 1).

88 Under the assumption of a steady-state ocean, which is supported by the relative constancy of climate and  
89 atmospheric CO<sub>2</sub> for centuries prior to the onset of the industrial revolution (~1800)<sup>17</sup>, the oceanic pool of  
90 natural CO<sub>2</sub> remains constant and the fluxes of natural CO<sub>2</sub> are globally balanced. This assumption permitted  
91 researchers already in the 1970s to use models and observations to determine the oceanic uptake of  
92 anthropogenic CO<sub>2</sub><sup>18-20</sup>, with subsequent work refining the methods and improving the data base<sup>2,4,15,21,22</sup>.

93 However, it has become increasingly clear since the 2000s that the natural carbon fluxes of the ocean are  
94 changing, and that the ocean sink for carbon is more variable<sup>23-32</sup>. The natural CO<sub>2</sub> pool is in fact highly

95 mobile, responding to changes in physical forcing from the atmosphere through changes in winds and in the  
96 fluxes of heat and freshwater, inducing changes in ocean circulation, temperature, salinity, and ocean  
97 biology<sup>9</sup>. Moreover, the anthropogenic CO<sub>2</sub> pool is more changeable than previously thought, responding to  
98 changes in atmospheric CO<sub>2</sub> growth rate or changes in ocean circulation<sup>33</sup>.

99 In this Review, we assess what is currently known about the ocean sink for CO<sub>2</sub>, and how it has responded to  
100 the rising CO<sub>2</sub> emissions in recent decades, relying primarily on ocean observations. We describe the  
101 variability of this sink and its drivers, which are debated. Finally, we highlight the need for increased  
102 observational capacity to support long term decision making, especially for the use of oceanic carbon dioxide  
103 removal (negative emission) approaches.

104

## 105 **[H1] OCEAN CARBON SINK TRENDS**

106

107 Since the late 1950s, the ocean has taken up a net  $25 \pm 2\%$  of the total anthropogenic CO<sub>2</sub> emissions<sup>1</sup>. This  
108 fractional uptake has remained relatively constant through time, meaning that the ocean sink tripled over  
109 these six decades, increasing from about  $-0.9 \text{ Pg C yr}^{-1}$  in the early 1960s to more than  $-3 \text{ Pg C yr}^{-1}$  in 2020<sup>1,25</sup>  
110 (note that the geophysical convention of fluxes being are considered positive here, so that an uptake of CO<sub>2</sub> is  
111 negative). This increasing ocean carbon sink is an ecosystem service that amounts to about 2 trillion Euros  
112 worth of emission reductions per year if valued at a typical marginal abatement cost compatible with a 1.5°C  
113 target of 200 Euro per ton of CO<sub>2</sub><sup>34</sup>. Together with the large ocean uptake of the excess heat generated from  
114 rising atmospheric CO<sub>2</sub><sup>35</sup>, the ocean has moderated the climate change experienced so far<sup>36,37</sup>. This section  
115 reviews how this ocean sink has been determined and what drives this long-term trend.

116

117

### 118 ***[H2] Response to rising atmospheric CO<sub>2</sub>***

119 The primary driver causing a long-term (> decades) change in the ocean's inventory of DIC is the rise in  
120 atmospheric CO<sub>2</sub>, driving a flux of anthropogenic CO<sub>2</sub> across the air-sea interface and then from the surface  
121 ocean to depth (Box 1). The rate limiting step for the uptake of anthropogenic CO<sub>2</sub> by the ocean is the  
122 transport from the surface to deeper layers<sup>38</sup>, as it takes decades to centuries for waters to circulate from the  
123 surface to the deeper ocean and back again<sup>39,40</sup>. In contrast, CO<sub>2</sub> gas exchange across the air-sea interface is  
124 comparably fast (e-folding time scale of less than a year<sup>9,41</sup>), so that the CO<sub>2</sub> concentration of the surface  
125 ocean follows the atmospheric perturbation relatively closely<sup>42-44</sup>, with the magnitude of increase determined  
126 by the surface **ocean's buffer (or Revelle) factor**<sup>9,45,46</sup> **[G]**. The two processes air-sea exchange and the  
127 surface-to-deep transport of CO<sub>2</sub> respond approximately linearly to changes in atmospheric CO<sub>2</sub>. However,  
128 there is some the moderate non-linearity owing to the ocean's decreasing buffering capacity due to **ocean**

129 **acidification [G]** (a decrease of about 10% since preindustrial times<sup>47</sup>) that needs to be taken into account as  
 130 well<sup>48,49</sup>.

131 When a (near)linear system like the ocean uptake of anthropogenic CO<sub>2</sub> ( $C_{\text{ant}}$ ) is forced exponentially with a  
 132 fixed growth rate (as is the case for atmospheric CO<sub>2</sub> since ~1970) (Fig 1a), all components of the system will  
 133 increase proportionally after an initial adjustment (which is about a decade<sup>50</sup>). This proportionality implies a  
 134 linear scaling between the forcing (atmospheric CO<sub>2</sub>) and the response (ocean accumulation of anthropogenic  
 135 CO<sub>2</sub>), which is confirmed by results from observations<sup>2,4</sup>, **ocean inverse models<sup>3</sup> [G]** and **forward simulations**  
 136 **[G]** with **ocean biogeochemical models<sup>25,51</sup> [G]** (Fig 1a). The slope of this relationship (the line in Fig 1a)  
 137 represents the carbon concentration feedback of the ocean<sup>52,53</sup> and is described as the sensitivity, where  $\beta =$   
 138  $\partial C_{\text{ant}} / \partial \Delta \text{CO}_2^{\text{a}}$ , with the exact value dependent on the forcing history and especially past atmospheric growth  
 139 rate. An emergent property of this relationship is that during periods of exponential growth in atmospheric  
 140 CO<sub>2</sub>, it directly determines the global oceanic uptake flux of anthropogenic CO<sub>2</sub> ( $F_{\text{ant}}(t)$ ) from the growth rate  
 141 of atmospheric CO<sub>2</sub>:  $dC_{\text{ant}}/dt = -F_{\text{ant}}(t) = \beta \cdot d\Delta \text{CO}_2^{\text{a}}/dt$ , where the negative sign in front of  $F_{\text{ant}}$  reflects the  
 142 convention of ocean uptake being negative.

143 This simple scaling relationship does not apply once the atmospheric CO<sub>2</sub> growth begins to deviate  
 144 substantially from an exponential, as is expected if emissions start to stabilize and decrease in response to  
 145 global efforts to curb climate change<sup>54</sup>. In such cases, more complete theories building on deconvolution  
 146 concepts such as pulse response functions<sup>3,55</sup> or transit time distributions (TTD)<sup>56-58</sup> are much better suited  
 147 to describe the oceanic uptake of anthropogenic CO<sub>2</sub><sup>59</sup>. Nevertheless, the high CO<sub>2</sub> concentration in the  
 148 atmosphere would still be the main driving force for the many centuries it takes to equilibrate the entire ocean  
 149 with the atmospheric perturbation.<sup>60</sup>

150

## 151 **[H2] Cumulative oceanic uptake**

152 The tight relationship between the ocean uptake for anthropogenic CO<sub>2</sub> and the growth in atmospheric CO<sub>2</sub>  
 153 was recognized by the 1970s<sup>18,61,62</sup>. However, until the mid-1980s, high-quality measurements of oceanic DIC  
 154 were extremely scarce<sup>63</sup>, making it impossible to constrain this relationship with observations. As the number  
 155 of reliable DIC measurements increased in the late 1970s methods to identify the anthropogenic CO<sub>2</sub> signal  
 156 within the substantial background variability of DIC emerged<sup>19,20</sup>. Since the data were typically available  
 157 only from a one-time survey, back-calculation approaches were used that implicitly assume a steady-state  
 158 ocean. In such approaches, the DIC concentration in a water parcel in the ocean's interior is traced back to its  
 159 origin at the surface, correcting along the way for the biological changes that incurred along this journey from  
 160 the surface to depth<sup>15,21</sup>. Refinement of the initial approaches led to the  $\Delta C^*$  method<sup>64,65</sup>, which is the most  
 161 widely used back-calculation method to identify the total amount of anthropogenic CO<sub>2</sub> that has accumulated

162 in the ocean since preindustrial times<sup>21</sup>. A crucial enabling development for the identification of the  
163 relatively small anthropogenic CO<sub>2</sub> signal (see also Box 1) was the introduction of common measurement  
164 methodologies<sup>66</sup> and certified reference materials<sup>67,68</sup> that permitted the collation of DIC measurements taken  
165 years apart and measured by different laboratories around the world into an internally coherent data set<sup>69</sup>.

166 The application of the  $\Delta C^*$  approach to the data collected by the Joint Global Ocean Flux Study  
167 (JGOFS)/World Ocean Circulation Experiment (WOCE) programs in the mid-1980s to mid-1990s led to the  
168 first global data-based estimate of the accumulation of anthropogenic CO<sub>2</sub><sup>2</sup>. This approach yielded a total  
169 anthropogenic CO<sub>2</sub> inventory for the nominal year 1994 of 118 ±19 Pg C (Fig 1a), i.e., reflecting the time  
170 integrated ocean uptake since ~1800. The maps in Fig 1b show the well-established spatial variations in the  
171 vertically integrated amount of anthropogenic CO<sub>2</sub><sup>38,70–72</sup> (Fig. 1b). Strong accumulation in the North Atlantic  
172 contrasts with regions of relatively low accumulation such as the Tropical Pacific and the polar Southern  
173 Ocean. One of the most conspicuous features of the spatial variation is the band of high accumulation north  
174 of the Southern Ocean between about 30°S to 40°S. These basin-scale differences are a direct consequence of  
175 the regional effectiveness with which anthropogenic CO<sub>2</sub> is transported from the surface downward into the  
176 ocean's interior<sup>70,72–74</sup>. The Ocean Inversion Project used such knowledge about the surface to depth  
177 transport in the form of impulse response functions, to estimate how much uptake of anthropogenic CO<sub>2</sub> is  
178 required in order to match the reconstructed distribution of anthropogenic CO<sub>2</sub> in 1994. This estimate yielded  
179 an uptake flux of  $-2.2 \pm 0.25$  Pg C yr<sup>-1</sup> for a nominal year 1995<sup>72</sup>.

180 This inventory also provided the first observation-based estimate of  $\beta$  of  $1.47 \pm 0.24$  Pg C / ppm CO<sub>2</sub>,  
181 representing the time period 1800-1994 (Supplementary Table 1). These results confirmed many prior  
182 estimates that so far had relied on models<sup>18,38,71</sup> or indirect constraints such as the changes in atmospheric  
183 oxygen<sup>75</sup> or budgets of the stable isotope of carbon (<sup>13</sup>C)<sup>76–78</sup>.

## 184 **[H2] Decadal trends in uptake**

185

186 The linear  $\beta$ -scaling can be used to provide a first estimate of the further evolution of the oceanic sink. Given  
187 the observed trend in the atmospheric CO<sub>2</sub> growth rate of 0.3 ppm yr<sup>-1</sup> decade<sup>-1</sup> between 1994 and 2007 and  
188 the inferred sensitivity  $\beta$  of  $1.47 \pm 0.24$  Pg C / ppm CO<sub>2</sub>, one would expect the steady-state ocean sink for  
189 anthropogenic CO<sub>2</sub> to increase (become more negative) by about  $-0.4$  Pg C decade<sup>-1</sup> over this period, yielding  
190 an uptake in 2007 of the order of  $-2.6$  Pg C yr<sup>-1</sup>. Forward and inverse models<sup>3,25,70,79</sup> have been used to assess  
191 this trend prediction (Fig 1a), but the ultimate evidence has to come from direct documentation of the  
192 increase in the ocean's DIC pool.

193 Direct documentation of decadal trends in anthropogenic CO<sub>2</sub> uptake is not straightforward, as shorter-term  
194 variations in the natural carbon pool tend to mask the slower but steadier increase in anthropogenic CO<sub>2</sub>. This  
195 problem can be overcome for regularly sampled timeseries<sup>43,80,81</sup>, but only a few sites have sufficient

196 observations to distinguish the anthropogenic trend from the natural variability. In most cases, the sampling  
197 rate is once per decade, as is the case for the GO-SHIP Global Repeat Hydrography Program<sup>82</sup>, for example.  
198 These data suffer acutely from an overprint of short-term variability in the natural carbon cycle, typically  
199 leading to a very noisy pattern of change that is difficult to interpret<sup>83</sup>.

200 The introduction of the extended multiple linear regression (eMLR) approach<sup>84</sup> enabled the change in  
201 anthropogenic CO<sub>2</sub> to be mostly isolated<sup>85,86</sup>. This method is the most widely used approach for detecting and  
202 quantifying changes in the anthropogenic CO<sub>2</sub> in the interior ocean based on repeat hydrography cruises<sup>83,87–</sup>  
203 <sup>89</sup>. Compared to the  $\Delta C^*$  approach, the eMLR approach captures both the steady-state and the non-steady-  
204 state accumulation of anthropogenic CO<sub>2</sub>, although with limited accuracy when reconstructing the non-  
205 steady-state component<sup>90</sup>.

206 A modified version of the eMLR method (eMLR(C\*) method<sup>90</sup>) was used to estimate the change in  
207 anthropogenic CO<sub>2</sub>,  $\Delta C_{\text{ant}}$ , globally<sup>4</sup>, using DIC and other biogeochemical data from the JGOFS/WOCE  
208 survey for the 1990s and comparing them with the measurements from the 2000s obtained during the 1<sup>st</sup>  
209 round of the GO-SHIP Repeat Hydrography Program<sup>82</sup> (Fig. 1c). Global ocean carbon storage was estimated<sup>4</sup>  
210 to increase by  $34 \pm 4$  Pg C between 1994 and 2007, bringing the total inventory for anthropogenic CO<sub>2</sub> for  
211 2007 to  $154 \pm 19$  Pg C (Fig 1a). This increase in storage corresponds to a mean ocean uptake flux of  
212 anthropogenic CO<sub>2</sub> of  $-2.6 \pm 0.3$  Pg C yr<sup>-1</sup> over the 1994 to 2007 period, corroborating the simple scaling  
213 prediction. It also suggests a sensitivity  $\beta$  of  $1.39 \pm 0.16$  Pg C / ppm CO<sub>2</sub>, which is statistically  
214 indistinguishable from that estimated from the anthropogenic CO<sub>2</sub> inventory in 1994 ( $1.47 \pm 0.24$  Pg C / ppm  
215 CO<sub>2</sub>, Supplementary Table 1). This lack of a difference provides strong support for the steady-state  
216 assumption.

217 Given this steady-state, the ocean interior estimate for 1994 to 2007 can be scaled to each decade over the  
218 past 30 years using  $\beta$ , yielding  $-2.1$  Pg C yr<sup>-1</sup> for 1990 to 1999,  $-2.6$  Pg C yr<sup>-1</sup> for the subsequent decade, and -  
219  $3.3$  Pg C yr<sup>-1</sup> for 2010 through 2019 (Table 1). Models suggest a smaller sensitivity  $\beta$ , lower mean uptake and  
220 smaller decadal trends (Table 1, Supplementary Table 1). However, many of the differences are not  
221 statistically significant, confirming that the ocean acts as a strong and increasing sink for anthropogenic CO<sub>2</sub>.  
222 Overall, the steady-state assumption is useful determining the multidecadal oceanic uptake of anthropogenic  
223 CO<sub>2</sub>. However, this assumption does not hold as well when analyzing shorter-term variations or spatial  
224 variations.

225

226 **[H2] Non-steady-state uptake**

227

228 A more detailed analysis of the spatial variations in the ocean interior accumulation of anthropogenic CO<sub>2</sub>  
229 highlights the limits of the steady-state assumption (Fig 1b,c). To first order, the increase in anthropogenic  
230 CO<sub>2</sub> is proportional to how much anthropogenic CO<sub>2</sub> was present at the beginning<sup>4,42,91</sup>. The proportionality  
231 can be estimated using the  $\beta$  approach, yielding a value of  $0.28 \pm 0.02$  for the inventory in 1994 and the change  
232 in inventory<sup>4</sup> between 1994 and 2007 (similar approaches using a transit-time distribution (TTD) approach<sup>57</sup>  
233 yield comparable results). Thus, differences in the scaled spatial distribution of  $C_{\text{ant}}$ (1994) (Fig 1b) and  
234  $\Delta C_{\text{ant}}$ (2007-1994) (Fig 1c) suggest a non-steady-state contribution. Although the uncertainties in the two  
235 reconstructions are substantial, they suggest a shift in the accumulation of anthropogenic CO<sub>2</sub> from the North  
236 Atlantic to the South Atlantic, potentially related to decadal shifts in the overturning circulation<sup>92</sup>. This  
237 pattern confirms the presence of substantial decadal variability in the ocean carbon cycle identified  
238 previously along basin-wide hydrographic sections that had been occupied multiple times<sup>83,89</sup>. However, the  
239 decadal nature of the repeat hydrography program limits the ability to constrain the year-to-year variability of  
240 the ocean carbon sink via the changes in the carbon storage.

241

## 242 [H1] OCEAN CARBON SINK VARIABILITY

243

244 Analyses of the sea-to-air fluxes of CO<sub>2</sub> are better suited to address this challenge, as they can be used to  
245 analyze changes at much higher temporal resolutions. In addition, they also assess the potential contribution  
246 of the non-steady-state component of the natural CO<sub>2</sub> fluxes, which we expect to drive most of the ocean flux  
247 variability. The ability to constrain these sea-to-air CO<sub>2</sub> fluxes with observations has made large strides in the  
248 last decade for at least three reasons. First was the expansion of the surface ocean **partial pressure of CO<sub>2</sub> [G]**  
249 (pCO<sub>2</sub>) measurement programs that began in the 1960s<sup>93</sup>, but picked up momentum in the late 1980s and  
250 1990s<sup>94-96</sup>. Second was the collation of the available surface ocean pCO<sub>2</sub> measurements by the Surface  
251 Ocean CO<sub>2</sub> Atlas (SOCAT) effort into a quality controlled and openly accessible data product<sup>97-99</sup>. More than  
252 30 million observations are in the [SOCAT](#) V2022 release, but these observations cover only a small fraction  
253 of the ocean surface. For example, at any given month in the decade of the 2010s, only 3% of all 1°x 1° grid  
254 points of the surface ocean have at least one observation. Therefore, the third notable advance was the  
255 development of approaches to inter- and extrapolate these surface ocean pCO<sub>2</sub> observations to obtain space-  
256 time continuous estimates of the sea-to-air CO<sub>2</sub> fluxes<sup>100-102</sup>. Six of these reconstructions have been  
257 harmonized into a globally consistent product<sup>103</sup>, called SeaFlux.

258 The long-term mean fluxes of this ensemble are characterized by strong outgassing of CO<sub>2</sub> in equatorial  
259 regions, most prominently in the equatorial Pacific (Fig 2). There is a strong net uptake of CO<sub>2</sub> at latitudes  
260 around 45° in both hemispheres. The overall pattern of the sources and sinks of CO<sub>2</sub> is primarily determined  
261 by the exchange of natural CO<sub>2</sub>, responding to heating and cooling, vertical transport and mixing, and



262 variations in biological productivity<sup>9</sup>. The uptake of anthropogenic CO<sub>2</sub> modifies these fluxes, most strongly  
 263 in the areas of large uptake of anthropogenic CO<sub>2</sub> such as the tropics and the high latitudes<sup>104</sup>.

264 There is an almost doubling of the global net sea-to-air flux of CO<sub>2</sub> estimated by the SeaFlux ensemble from -  
 265 1.5 Pg C yr<sup>-1</sup> in 1990 to -2.7 Pg C yr<sup>-1</sup> in 2018 (Fig. 3a). A loss of natural CO<sub>2</sub> of  $0.65 \pm 0.30$  Pg C yr<sup>-1</sup><sup>105</sup>  
 266 needs to be subtracted from the pCO<sub>2</sub> based estimates to compare these net fluxes with the global ocean  
 267 uptake estimates here (Table 1) and also those reported by the Global Carbon Project<sup>1,51</sup>. This loss is part of a  
 268 natural steady-state of the global carbon cycle, and results from the difference between the carbon input by  
 269 rivers and the carbon burial in marine sediments<sup>105–108</sup> (see also Box 1). Based on this information, the  
 270 combined fluxes of steady-state anthropogenic CO<sub>2</sub> and non-steady-state natural and anthropogenic CO<sub>2</sub> of -  
 271  $2.1 \pm 0.3$  Pg C yr<sup>-1</sup> in the 1990s,  $-2.3 \pm 0.2$  Pg C yr<sup>-1</sup> in the 2000s, and  $-3.1 \pm 0.2$  Pg C yr<sup>-1</sup> in the 2010s (Table 1)  
 272 (this flux is referred to as the ocean sink S<sub>OCEAN</sub> in the Global Carbon Budget<sup>1,51</sup>).

273

## 274 **[H2] Interannual to decadal variability**

275 The overall trend from the 1990s to the present of about  $-0.4$  Pg C yr<sup>-1</sup> decade<sup>-1</sup> is close to that estimated from  
 276 the steady-state model for anthropogenic CO<sub>2</sub> (orange dashed line in Fig 3a). The simulated fluxes from a  
 277 model run with constant circulation and constant biology (CESM-ETHZ)<sup>25</sup> show the same overall trend (red  
 278 dashed line), although with some more variations, largely reflecting changes in the growth rate of  
 279 atmospheric CO<sub>2</sub><sup>33</sup>. Thus, when analyzed over the last three decades, the surface ocean fluxes suggest an  
 280 ocean carbon sink that has increased at a rate commensurate with the steady-state prediction.

281 However, on interannual to decadal timescales, the ocean carbon sink diagnosed from the surface pCO<sub>2</sub>  
 282 observations deviates substantially from the steady-state prediction (Fig 3a). The strongest deviations occur  
 283 on decadal timescales, with a weakening sink during the 1990s (a decadal trend of  $+0.3$  Pg C yr<sup>-1</sup> decade<sup>-1</sup>  
 284 (1990-2001)), followed by a strong reinvigoration with a decadal trend of  $-0.7$  Pg C yr<sup>-1</sup> decade<sup>-1</sup> (2002-  
 285 2018), nearly twice the rate from the steady state model. Integrated over the three decades, the ensemble  
 286 mean uptake is  $6 \pm 5$  Pg C (11%) smaller than expected from the steady-state prediction, that is, this difference  
 287 suggests a non-steady-state or climate variability induced loss of natural and anthropogenic CO<sub>2</sub>. The  
 288 estimates from the individual pCO<sub>2</sub>-based reconstructions (shown in grey in Fig 3a) vary substantially around  
 289 the SeaFlux ensemble mean, but all agree on the strong decadal modulation of the ocean carbon sink around  
 290 the long-term trend.

291 All ocean basins contribute to the decadal variations of the ocean carbon sink, but the largest changes occur  
 292 in the Pacific Ocean and the Southern Ocean, which is defined here as the ocean south of 44°S<sup>24,32,109,110</sup> (Fig  
 293 3b). Both basins experienced a strong minimum in uptake around 2002 and a recovery thereafter, while the  
 294 Atlantic basin north of 44°S had a more gradual increase through time. The Pacific is the only basin that

295 exhibits a clear interannual variability signal on top of the trend and the decadal changes. In contrast, the  
296 carbon sink of the Indian Ocean north of 44°S remained relatively constant.

297 Given that all these estimates rely on the same sparsely sampled ocean pCO<sub>2</sub> data, though, the potential for  
298 systematic errors that transcends all interpolation methods cannot be excluded<sup>111</sup>. The reconstructions in the  
299 Southern Hemisphere are particularly concerning, as model based analyses<sup>111</sup> suggest that the severe  
300 undersampling could lead to an overestimating of the diagnosed decadal variability. In addition, the cool  
301 surface ocean skin effect<sup>112</sup> and uncertainties associated with the functional dependence of the gas transfer  
302 velocity on wind and other environmental factors<sup>113</sup> add to the overall uncertainty of the flux products.  
303 Regardless, these variations—especially the weakening and strengthening periods—are seen in other,  
304 independent estimates, including from forward models<sup>25</sup> and inverse models<sup>114</sup>, although with generally  
305 smaller magnitudes<sup>23</sup>.

306

307

## 308 **[H2] Patterns of variability**

309 More details about the spatio-temporal nature of the sea-to-air flux variations can be gleaned from the pCO<sub>2</sub>  
310 observation-based constraints that emerged in the 2010s. A Hovmoeller plot of the zonal integrals of the  
311 anomalous air-sea fluxes (Fig 4a) shows that the largest variations occur in the regions of strong absolute  
312 fluxes, that is, either in regions of strong uptake (temperate to high latitudes) or in the regions of strong  
313 outgassing of CO<sub>2</sub> (tropics). On top of the year-to-year variations, which are most prominent in the tropical  
314 latitudes, the long-term changes and the superimposed decadal variability clearly emerge from the data. They  
315 indicate that the extratropics (between 30° and 60° latitude) were the most important latitudes contributing to  
316 the rapid growth in the ocean carbon sink in the 2000s and 2010s, with the southern hemisphere dominating  
317 due to its larger ocean surface area.

318 These fluxes are the sum of the anomalies of the anthropogenic and natural CO<sub>2</sub> flux components. To  
319 separate them, the Ocean Inversion Project-based steady-state estimates for the uptake of anthropogenic CO<sub>2</sub>  
320 from the<sup>72</sup> for the year 1995 were scaled to the entire period using the  $\beta$ -based scaling approach used above.  
321 The zonal integral of the anomalies of this steady-state component of the anthropogenic CO<sub>2</sub> flux indicates  
322 that the regions of highest uptake in the Southern Ocean, the tropics and the mid latitudes of the northern  
323 hemisphere imprint large trends on the fluxes in these regions. In contrast, other regions have only a small  
324 trend in absolute terms (Fig 4b).

325 By removing this anthropogenic steady-state trend from the anomalous flux, the remaining anomalies reveal a  
326 clearer picture of the non-steady-state components driven by climate variability (Fig 4c). The strong  
327 interannual nature of the variations in the tropical belt emerges even more prominently. These anomalies are

328 correlated to the El Niño Southern Oscillation (ENSO) [G], as indicated by the negative correlation of the  
329 zonal anomalies in the tropical belt with the multivariate ENSO index<sup>115</sup> ( $R = -0.79$ ,  $p < 0.05$ ). However, the  
330 anomalous uptake during El Niños was strong in the 1990s and weakened substantially after the turn of the  
331 millennium. At the same time, the anomalous outgassing during La Niña conditions strengthened over time.  
332 These ENSO related trends yield a distinct decadal signal in the tropics as well, characterized by an  
333 anomalous uptake during the 1990s, neutral conditions during the first decade of the new millennium, and  
334 anomalous outgassing in the 2010s.

335 The decadal nature of the Southern Ocean sink variability is also more discernible in these non-steady-state  
336 fluxes (Fig 4c). Over the course of the 1990s, there was a rapid change from an anomalous uptake to an  
337 anomalous outgassing peaking around 2002. This was followed by a prolonged period of anomalous  
338 outgassing until about 2008 and a recovery to normal conditions around 2010. Thus, the strong trend in the  
339 Southern Ocean toward increasing uptake in the last two decades is largely the result of the strong trend  
340 imparted by the steady-state uptake of anthropogenic CO<sub>2</sub>, reflecting the major role of the this region in  
341 taking up anthropogenic CO<sub>2</sub> from the atmosphere (Fig 4b)<sup>72,116</sup>.

342 The trend from an anomalous sink to an anomalous source during the 1990s followed by a strengthening  
343 period after 2000 is also evident across most latitudes of the northern hemisphere (Fig 4c). This co-  
344 occurrence suggests that apart from the tropics, the decadal mode of sea-to-air CO<sub>2</sub> flux variability has a  
345 global component, even after accounting for the steady-state trend in the uptake flux of anthropogenic CO<sub>2</sub>.

346 In summary, the pCO<sub>2</sub> observation-based constraints on the sea-to-air CO<sub>2</sub> fluxes that have emerged in the  
347 last decade have reshaped our understanding of the variability of the ocean carbon sink (Figure 5). In  
348 particular, the surface flux products have suggested the presence of an important decadal mode of variability  
349 in the extra-tropics, and particularly in the Southern Ocean (Figure 5). This observation contrasts with the  
350 results of ocean biogeochemical models, whose variability tend to be, on average, smaller, and also which  
351 tend to have most of the variability focused in the tropics<sup>25,30,117</sup>. Nevertheless, the models also simulate  
352 decadal variability in the extratropics<sup>23,25,28,29,118</sup>), adding further evidence that the decadal variability  
353 diagnosed from the observations is a robust feature.

354

## 355 ***[H2] Mechanisms of variability***

356  
357 Variations in the ocean carbon sink can either be caused by processes that are internal to the climate system  
358 or can be externally forced. Internal forcing is associated with variations in weather and climate  
359 <sup>24,27,28,32,109,114,119</sup> including changes associated with anthropogenic climate change<sup>120</sup>. Externally forced  
360 variations are caused by changes outside the climate system, such as those induced by the volcanic eruption

361 of Mount Pinatubo in 1991<sup>33</sup>. Such an eruption can impact the ocean carbon sink through changes in both  
362 Earth surface temperature and atmospheric CO<sub>2</sub> growth rate.

363 Interannual variations in the ocean carbon sink are driven by internal processes, as they are associated with  
364 the ENSO-related year-to-year variations in the sea-to-air fluxes in the tropical Pacific<sup>30,121–123</sup>. During El  
365 Niño conditions, reduced upwelling and thermocline deepening in the Eastern Tropical Pacific strongly  
366 decrease the vertical supply of DIC to the surface. This process causes a collapse of the high pCO<sub>2</sub> levels that  
367 drive CO<sub>2</sub> out of the ocean, even though sea-surface temperatures are warmer than normal. Reduced  
368 windspeeds during El Niño conditions tend to further reduce the outgassing and thus enhance the effect of the  
369 reduced supersaturation<sup>123</sup>. The resulting sea-to-air flux anomalies are sizable and impact the regional  
370 atmospheric CO<sub>2</sub> concentration<sup>124</sup>. The flux variations are most likely almost entirely driven by changes in  
371 the natural CO<sub>2</sub>, in particular its non-steady-state component (Fig 4c).

372 Mechanisms driving the decadal variations in the ocean carbon sink are less understood. One argument is that  
373 at least part of the variations are externally forced<sup>33</sup>, as the eruption of Mt Pinatubo in 1991 caused both a  
374 reduced growth rate of atmospheric CO<sub>2</sub> during much of the 1990s<sup>125–127</sup> and a global cooling trend in the  
375 surface temperature. The low growth rate reduces the ocean carbon sink directly by modifying the air-sea  
376 pCO<sub>2</sub> gradient. This effect would be enhanced by the upper ocean cooling and the associated enhanced ocean  
377 mixing caused by the global cooling<sup>128,129</sup>. According to this argument, these two processes would have  
378 reduced the oceanic uptake during the 1990s, while the resumption of higher atmospheric CO<sub>2</sub> growth rates  
379 thereafter would have caused the ocean uptake to rebound<sup>33</sup>.

380 An alternative line of arguments is that these decadal changes are the result of processes that are internal to  
381 the climate system. For example, a poleward contraction and intensification of the westerly wind belt around  
382 Antarctica might have caused the weakening trend of the Southern Ocean carbon sink during the 1990s<sup>28</sup>,  
383 driven primarily by a trend toward a positive phase of the **Southern Annular Mode [G]** (SAM)<sup>130</sup>. The  
384 stronger winds led to more upwelling of CO<sub>2</sub> and nutrient rich deep water, increasing CO<sub>2</sub> outgassing (albeit  
385 partly balanced by stronger biological production)<sup>28,118,131,132</sup>. Then, a shift to a zonally more undulating  
386 windfield coupled with changes in sea-surface temperature caused the reinvigoration of the Southern Ocean  
387 carbon sink thereafter<sup>32</sup>. At least a part of these wind changes, and especially those of the 1990s, have been  
388 attributed to anthropogenic warming and ozone loss forcing the positive trend in the SAM<sup>133</sup>. Simulations  
389 suggest that the majority of the response of the CO<sub>2</sub> fluxes is driven by changes in the natural CO<sub>2</sub>  
390 component, with the fluxes of anthropogenic CO<sub>2</sub> modulating the response, often in opposite directions, thus  
391 moderating the effect<sup>24,28,114,132</sup>.

392 In contrast to the Southern Ocean, the potential mechanisms causing the reconstructed increases in the carbon  
393 sink in the northern hemisphere after 2000 are not well investigated. They most likely mechanisms involve  
394 changes in winds, changes in temperature affecting the solubility, changes in buoyancy forcing affecting

395 winter mixed layers<sup>134</sup>, and large-scale gyre changes<sup>27</sup>. The latter are potentially associated with changes in  
396 the northern annular mode (NAM) or associated northern hemisphere modes of variability<sup>109</sup>.

397 The relative roles of internal versus external forcing driving the reconstructed decadal variations still need to  
398 be firmly established. Simulations with a changing atmospheric CO<sub>2</sub> growth rate, but no changes in climate,  
399 suggest that the effect is visible, albeit much smaller than the observed changes (the dashed red versus orange  
400 line in Fig 3a). The effect of the cooling and warming pattern associated with Mt. Pinatubo is more difficult  
401 to quantify independently, but simulations with comprehensive **ocean biogeochemical models [G]**<sup>128,135</sup>  
402 suggest an effect  $\leq 0.2$  Pg C yr<sup>-1</sup> during peak cooling, and rapidly decreasing thereafter. However, the ocean  
403 carbon sinks changing globally relatively synchronously supports that there was an external forcing  
404 mechanism (Fig 4). Overall, external forcing (such as by volcanos) and internal changes (as by weather and  
405 climate variability) are not mutually exclusive processes, and both likely play a role in driving ocean carbon  
406 sink variability.

407

## 408 **[H2] Merging observational constraints**

409 Bringing together the ocean interior constraints on the evolution of the ocean sink with those provided by the  
410 surface ocean measurements can help to better understand the mechanisms driving trends and variability  
411 (Table 1). The estimates of the ocean interior accumulation of anthropogenic CO<sub>2</sub> suggest an ocean that  
412 globally has operated near steady-state. The extrapolation with  $\beta$ -scaling suggests a cumulative uptake of  
413 about 83 Pg C between 1990 and 2018. The reconstructions of the surface fluxes, which include both natural  
414 and anthropogenic CO<sub>2</sub> components, suggest  $6 \pm 5$  Pg C less uptake over the same period (Table 1, Fig 3a).  
415 This reduction is mostly attributed to a non-steady-state loss of natural CO<sub>2</sub>, as the simulation with the  
416 observed variations in atmospheric CO<sub>2</sub> suggested a small change in the total uptake of anthropogenic CO<sub>2</sub>  
417 (red versus orange dashed lines in Fig 3). This loss needs to be taken into consideration when constructing  
418 global carbon budgets with ocean interior inventory changes. Indeed, a potential loss of  $5 \pm 3$  Pg C was  
419 considered in the global assessment of the accumulation of anthropogenic CO<sub>2</sub> for the period 1994 through  
420 2007<sup>4</sup>. In addition to circulation driven decadal variability, a part of this loss could be caused by ocean  
421 warming, as a warming induced loss of  $5 \pm 1$  Pg C between 1990 and 2000<sup>136</sup> has been suggested (Table 1).  
422 These losses and the corresponding budget adjustments are currently very tentative, and urgently require  
423 verifications through direct observations of changes in the oceanic DIC pool, for example.

424 While ocean interior and surface ocean constraints are becoming more consistent, new discrepancies have  
425 arisen. Most prominent is a growing difference between the ocean sink estimates based on surface ocean  
426 pCO<sub>2</sub> observations and those based on ocean biogeochemical models. These estimates agree well during the  
427 first decade of the millennium, but diverge thereafter, with the observation-based estimates indicating a much

428 larger growth in the uptake than the models<sup>1,25</sup> (Table 1). This difference is also evident in these models  
429 yielding a relatively low sensitivity  $\beta$  of  $1.11 \pm 0.18$  Pg C / ppm CO<sub>2</sub> for the period 1990 through 2018 (Fig 1a,  
430 Supplementary Table 1). One reason is that the presently used models tend to underestimate the uptake of  
431 anthropogenic CO<sub>2</sub>, as evidenced by direct comparison with the uptake estimates stemming from the  
432 accumulation of anthropogenic CO<sub>2</sub> (Fig 1b,c)<sup>1</sup>. A model-based emergent constraint approach on a different,  
433 but related set of models suggests an underestimation of about 10%<sup>137</sup>. Adjusting the models for this bias  
434 halves the mismatch between models and observations-based estimates for the period after 2010, but opens  
435 larger discrepancies in the earlier decades. The uncertainties in the observation-based flux products stemming  
436 from the sparse observations, and issues at the tails of the observational-based time-series<sup>112</sup> might contribute  
437 to these discrepancies.

438

### 439 **[H1] SUMMARY AND FUTURE PERSPECTIVES**

440 The strength of the ocean carbon sink has tripled from the 1960s until the present. Thus, the ocean has  
441 maintained its key role as a sink for the CO<sub>2</sub> emitted into the atmosphere as a consequence of human  
442 activities, removing about  $25 \pm 2\%$  of the total emissions over six decades. The strengthening of the ocean sink  
443 has been largely driven by the increasing uptake of anthropogenic CO<sub>2</sub> in response to the rise in atmospheric  
444 CO<sub>2</sub>, leading to a strong proportionality between the two. In contrast, the contribution from changes in the  
445 natural carbon cycle has been small so far, consistent with the assumption that the ocean circulation and  
446 biological pump was overall in steady-state. However, new insights and observations in the past decade  
447 challenge this assumption, especially on shorter timescales, suggesting an ocean that is more variable than  
448 previously recognized. New evidence also suggests over the past three decades a loss of natural CO<sub>2</sub> to the  
449 atmosphere due to ocean warming and changes in ocean circulation. If confirmed, such a loss suggests an  
450 ocean carbon sink that is rather vulnerable to climate change.

451 An ocean sink that is more vulnerable to climate change than currently assumed in coupled carbon-climate  
452 models<sup>52</sup> would imply that the ocean will take up less CO<sub>2</sub> from the atmosphere in the future than anticipated.  
453 This would leave a larger fraction of the emissions in the atmosphere, causing additional global warming and  
454 climate change. In other words, the ocean carbon-climate feedback could be more positive than suggested by  
455 current coupled carbon-climate models. Moreover, the finding of the ocean sink potentially being more  
456 sensitive to changes in atmospheric CO<sub>2</sub> growth rates than previously recognized, implies a stronger than  
457 anticipated decline of the ocean carbon sink in ambitious mitigation scenarios<sup>34,138</sup>.

458 The implications are large and far-reaching. Any reduction in ocean carbon uptake compared to current  
459 assumptions would require even stronger investments into decarbonization strategies, making the  
460 achievement of specific global warming targets harder. It also reduces the efficacy of the negative emission

461 approaches that aim to curb climate change by removing CO<sub>2</sub> from the atmosphere using land-based<sup>139,140</sup> or  
462 ocean-based<sup>141</sup> approaches.

463 To better constrain and predict the ocean carbon sink, there are three important challenges to address: the  
464 robustness of the reconstructed changes and variations; the processes driving these changes and variations;  
465 and predictions of the future ocean uptake, in particular the response of the ocean carbon sink to future  
466 climate change, the reduction in anthropogenic CO<sub>2</sub> emissions, and the potential deployment of carbon  
467 dioxide removal technologies. Addressing these challenges is important both scientifically and for policy. For  
468 example, during the upcoming Global Stocktake undertaken within the U.N. Framework Convention on  
469 Climate Change (UNFCCC), reliable estimates of the ocean carbon sink will be a crucial element to close the  
470 global carbon budget. In addition, the study of ocean-based carbon dioxide removal approaches, such as  
471 ocean alkalization, nutrient fertilization, seaweed growth, and artificial upwelling, have gained  
472 momentum<sup>141</sup>, requiring a thorough assessment of their effectiveness and consequences.

473 In our view, the following measures must be taken to answer these challenges (see also Ref<sup>142</sup>). The existing  
474 observation networks need to be improved, expanded, and put on a much better long-term funding level. The  
475 limited sampling of the ocean carbon system is currently the largest source of uncertainty in assessing the  
476 variability of the ocean carbon sink. The current sampling is sufficient to capture the long-term time mean  
477 sink, and the year-to-year variations in the tropical Pacific and a few other regions, especially in the northern  
478 hemisphere where the sampling is relatively dense. In contrast, sampling is critical in many other key regions,  
479 such as the Southern Ocean, the South Pacific and the Indian Ocean. Higher resolution observations in time  
480 and space will also help to better understand the processes leading to these variations, including those that  
481 lead to extremes in ocean acidification and/or deoxygenation<sup>143</sup>. Ocean observing system simulation  
482 experiments can help to determine where and when the observing density has to be increased, and to suggest  
483 optimal combinations of different observing platforms<sup>144,145</sup>.

484 To support observation, new technologies—especially those that enhance the ability to observe ocean carbon  
485 in an autonomous manner—need to be developed, improved, and strategically deployed. Improvement of  
486 analytical techniques, sensor technology and calibration methods for ocean carbon measurements is urgently  
487 required for the provision of accurate, well-calibrated ocean carbon measurements, while improving the ease  
488 and efficiency of data collection, thus increasing the scope for autonomous data collection and reducing the  
489 cost of these measurements, such as the Biogeochemical Argo program<sup>146–148</sup>.

490 To build on expanded and improved sampling, the existing ocean carbon synthesis projects (GLODAP and  
491 SOCAT) and the downstream efforts such as the Global Carbon Budget (GCB) and SeaFlux need to be  
492 strengthened and expanded. A more rapid update of the analyses, such as on a semi-annual basis providing  
493 closer to real-time analyses of the global carbon budget, could be useful to better linking the ocean to the

494 Global Stocktake activities. Similarly, models and observations need to be better integrated, especially  
495 through data assimilation and interpolation approaches<sup>149–151</sup>. As part of this effort, these models should be  
496 pushed to resolve smaller spatial and temporal scales, better capturing the small-scale variability that is  
497 inherent in the data that is collected and assimilated by these models. If these models can resolve both the  
498 large scales that are representative of global budgets, and the small scales that are representative of the  
499 observations, they will be able to more accurately reflect our state of knowledge and its uncertainty.

500  
501 Moving beyond carbon measurements and budgets, focused process studies need to be developed to better  
502 understand critical processes. The need to improve knowledge of the sensitivity of ocean biology to changes  
503 in temperature, ocean acidification and other parameters is pressing. In addition researchers need a better  
504 understanding of the aquatic continuum<sup>105</sup>—the aquatic network that connects the land aquatic systems to the  
505 ocean, delivering inorganic and organic matter to the ocean, whose fate is critical to determine the outgassing  
506 of river-derived CO<sub>2</sub>. Although a value of 0.65 Pg C yr<sup>-1</sup> for the degassing of terrestrially-derived CO<sub>2</sub> was  
507 used here and in the Global Carbon Budget<sup>1</sup>, individual estimates range between 0.2 Pg C yr<sup>-1</sup><sup>152</sup> and 1.2 Pg  
508 C yr<sup>-1</sup><sup>153</sup>, reflecting the large uncertainty of this estimate. An especially under-investigated area is the fate of  
509 the river-derived carbon in the ocean, and in particular, the determination of how much carbon is buried in  
510 sediments close to the river mouths, how much enters the open ocean and how fast this carbon is  
511 remineralized back to CO<sub>2</sub><sup>152</sup>.

512 The role of the ocean in taking up additional CO<sub>2</sub> in response to the deployment of carbon dioxide removal  
513 technologies needs to be critically evaluated. There must be a particular focus on the efficacy of these  
514 measures and their potential for negative (unintended) consequences<sup>154</sup>. Historically, the ocean sink for  
515 carbon has been considered as very robust to changes, and largely tracking the increase in atmospheric CO<sub>2</sub>.  
516 It is time to change this perspective and to recognize that the ocean carbon cycle might be more sensitive to  
517 change than previously recognized. The size of this sink, its unknown response to a reduction in  
518 anthropogenic CO<sub>2</sub> emissions and its relevance for past and future climates are large enough to warrant  
519 renewed efforts to observe it, to study it, and to understand it.

520  
521



522 **References**

523

524

525 *Top references*

526 **(1) Friedlingstein et al. (2022)**

527 **Most recent version of the Global Carbon Budget, an international effort led by the Global Carbon**  
528 **Project to synthesize all components of the global carbon cycle.**

529

530 **(2) Sabine et al. (2004)**

531 **First observation-based global inventory of anthropogenic CO<sub>2</sub> providing a key constraint for the**  
532 **global anthropogenic CO<sub>2</sub> budget.**

533

534 **(3) Khatiwala et al. (2009)**

535 **Reconstruction of the entire history of the oceanic uptake of anthropogenic CO<sub>2</sub>.**

536

537 **(4) Gruber et al. (2019)**

538 **Inventory of anthropogenic CO<sub>2</sub> that provided a second time-point describing the accumulation of**  
539 **anthropogenic CO<sub>2</sub> in the ocean based on ocean interior observations.**

540

541 **(25) Hauck et al. (2020)**

542 **Description and assessment of the ocean biogeochemical models currently used to determine the**  
543 **oceanic uptake of CO<sub>2</sub> in the context of the Global Carbon Budget.**

544

545 **(30) Le Quéré et al., (2007)**

546 **First study to point out that the Southern Ocean carbon sink weakened substantially during the 1990s.**

547

548

549 **(32) Landschützer et al. (2016)**

550 **Assessment of the decadal variability of the ocean carbon sink that reveals it is driven by the**  
551 **extratropical latitudes in both hemispheres.**

552

553 **(72) Mikaloff-Fletcher et al. (2006)**

554 **Ocean inversion-based study describing the regional distribution of the air-sea fluxes of anthropogenic**  
555 **CO<sub>2</sub> and its oceanic transport.**

556

557

558

559

560 *References by number:*

- 561
- 562 1. Friedlingstein, P. *et al.* Global Carbon Budget 2021. *Earth Syst. Sci. Data* **14**, 1917–2005 (2022).
- 563 2. Sabine, C. L. *et al.* The Oceanic Sink for Anthropogenic CO<sub>2</sub>. *Science* (80-. ). **305**, 367–371 (2004).
- 564 3. Khatiwala, S., Primeau, F. & Hall, T. Reconstruction of the history of anthropogenic CO<sub>2</sub>
- 565 concentrations in the ocean. *Nature* **462**, 346–349 (2009).
- 566 4. Gruber, N. *et al.* The oceanic sink for anthropogenic CO<sub>2</sub> from 1994 to 2007. *Science* (80-. ). **363**,
- 567 1193–1199 (2019).
- 568 5. Revelle, R. Introduction: The scientific history of carbon dioxide. in *The Global Carbon Cycle and*
- 569 *atmospheric CO<sub>2</sub>: Natural Variations Archean to Present* (eds. Sundquist, E. T. & Broecker, W. S.)
- 570 1–4 (AGU, 1985).
- 571 6. Heimann, M. A review of the contemporary global carbon cycle and as seen a century ago by
- 572 Arrhenius and Høgbom. *Ambio* **26**, 17–24 (1997).
- 573 7. Arrhenius, S. *Lehrbuch der kosmischen Physik*. **2**, (Hirzel, 1903).
- 574 8. Archer, D., Kheshgi, H. & Maier-Reimer, E. Multiple timescales for neutralization of fossil fuel CO<sub>2</sub>.
- 575 *Geophys. Res. Lett.* **24**, 405–408 (1997).
- 576 9. Sarmiento, J. L. & Gruber, N. *Ocean Biogeochemical Dynamics*. (Princeton University Press, 2006).
- 577 10. Callendar, G. S. The artificial production of carbon dioxide and its influence on climate. *Q. J. R.*
- 578 *Meteor. Soc.* **64**, 223–240 (1938).
- 579 11. Revelle, R. & Suess, H. E. Carbon Dioxide Exchange between Atmosphere and Ocean and the
- 580 question of an increase of atmospheric {CO<sub>2</sub>} during the past decades. *Tellus* **9**, 18–27 (1957).
- 581 12. Revelle, R., Broecker, W. S., Craig, H., Keeling, C. D. & Smagorinsky, J. *Atmospheric Carbon*
- 582 *Dioxide*. (1965).
- 583 13. Charney, J. G. *et al.* *Carbon Dioxide and Climate: A scientific assessment*. (1979).
- 584 14. Keeling, C. D. The concentration and isotopic abundances of carbon dioxide in the atmosphere. *Tellus*
- 585 **12**, 200–203 (1960).
- 586 15. W.R.Wallace, D. Chapter 6.3 Storage and transport of excess CO<sub>2</sub> in the oceans:The JGOFS/WOCE
- 587 global CO<sub>2</sub> survey. in *Ocean circulation and climate* (eds. Siedler, G., Church, J. & Gould, J.) 489–L
- 588 (Academic Press, 2001). doi:10.1016/S0074-6142(01)80136-4
- 589 16. Keppler, L., Landschützer, P., Gruber, N., Lauvset, S. K. & Stemmler, I. Seasonal Carbon Dynamics
- 590 in the Near-Global Ocean. *Global Biogeochem. Cycles* **34**, (2020).
- 591 17. Canadell, P. G. *et al.* Global Carbon and other Biogeochemical Cycles and Feedbacks. in *Climate*
- 592 *Change 2021: The Physical Science Basis. Contribution of Working Group I to the Sixth Assessment*
- 593 *Report of the Intergovernmental Panel on Climate Change* 673–816 (2021).
- 594 doi:10.1017/9781009157896.007
- 595 18. Oeschger, H., Siegenthaler, U., Schotterer, U. & Gugelmann, A. A box diffusion model to study the
- 596 carbon dioxide exchange in nature. *Tellus* **27**, 168–192 (1975).
- 597 19. Brewer, P. G. Direct observation of the oceanic {CO<sub>2</sub>} increase. *Geophys. Res. Lett.* **5**, 997–1000
- 598 (1978).
- 599 20. Chen, C.-T. A. & Millero, F. J. Gradual increase of oceanic CO<sub>2</sub>. *Nature* **277**, 205–206 (1979).
- 600 21. Sabine, C. L. & Tanhua, T. Estimation of Anthropogenic CO<sub>2</sub> Inventories in the Ocean. *Ann. Rev.*
- 601 *Mar. Sci.* **2**, 175–198 (2010).
- 602 22. Olsen, A. *et al.* The Global Ocean Data Analysis Project version 2 (GLODAPv2) – an internally
- 603 consistent data product for the world ocean. *Earth Syst. Sci. Data* **8**, 297–323 (2016).
- 604 23. DeVries, T. *et al.* Decadal trends in the ocean carbon sink. *Proc. Natl. Acad. Sci.* **116**, 201900371
- 605 (2019).
- 606 24. Gruber, N., Landschützer, P. & Lovenduski, N. S. The Variable Southern Ocean Carbon Sink. *Ann.*
- 607 *Rev. Mar. Sci.* **11**, 159–186 (2019).
- 608 25. Hauck, J. *et al.* Consistency and Challenges in the Ocean Carbon Sink Estimate for the Global Carbon
- 609 Budget. *Front. Mar. Sci.* **7**, 1–33 (2020).
- 610 26. Landschützer, P., Gruber, N., Bakker, D. C. E. & Schuster, U. Recent variability of the global ocean

- 611 carbon sink. *Global Biogeochem. Cycles* **28**, 927–949 (2014).
- 612 27. Landschützer, P., Gruber, N. & Bakker, D. C. E. Decadal variations and trends of the global ocean  
613 carbon sink. *Global Biogeochem. Cycles* **30**, 1396–1417 (2016).
- 614 28. Le Quere, C. *et al.* Saturation of the Southern Ocean CO<sub>2</sub> Sink Due to Recent Climate Change.  
615 *Science (80-. )*. **316**, 1735–1738 (2007).
- 616 29. Lovenduski, N. S., Gruber, N., Doney, S. C. & Lima, I. D. Enhanced CO<sub>2</sub> outgassing in the Southern  
617 Ocean from a positive phase of the Southern Annular Mode. *Global Biogeochem. Cycles* **21**, n/a-n/a  
618 (2007).
- 619 30. Le Quéré, C., Orr, J. C., Monfray, P., Aumont, O. & Madec, G. Interannual variability of the oceanic  
620 sink of CO<sub>2</sub> from 1979 through 1997. *Global Biogeochem. Cycles* **14**, 1247–1265 (2000).
- 621 31. Fay, A. R. & McKinley, G. A. Global trends in surface ocean p CO<sub>2</sub> from in situ data. *Global*  
622 *Biogeochem. Cycles* **27**, 541–557 (2013).
- 623 32. Landschützer, P. *et al.* The reinvigoration of the Southern Ocean carbon sink. *Science (80-. )*. **349**,  
624 1221–1224 (2015).
- 625 33. McKinley, G. A., Fay, A. R., Eddebbar, Y. A., Gloege, L. & Lovenduski, N. S. External Forcing  
626 Explains Recent Decadal Variability of the Ocean Carbon Sink. *AGU Adv.* **1**, 1–10 (2020).
- 627 34. Rogelj, J. *et al.* Mitigation Pathways Compatible with 1.5°C of Sustainable Development. in *Global*  
628 *warming of 1.5°C. An IPCC Special Report [...]* 93–174 (2018).
- 629 35. Cheng, L. *et al.* Another Record: Ocean Warming Continues through 2021 despite La Niña  
630 Conditions. *Adv. Atmos. Sci.* (2022). doi:10.1007/s00376-022-1461-3
- 631 36. Abram, N. *et al.* Chapter 1: Framing and Context of the Report. in *Special Report on the Ocean and*  
632 *Cryosphere (SROCC)* (eds. Pörtner, H.-O. *et al.*) (2019).
- 633 37. Bindoff, N. L. *et al.* Chapter 5: Changing Ocean, Marine Ecosystems, and Dependent Communities.  
634 in *Special Report on the Ocean and Cryosphere (SROCC)* (eds. Pörtner, H.-O. *et al.*) (2019).
- 635 38. Sarmiento, J. L., Orr, J. C. & Siegenthaler, U. A perturbation Simulation of CO<sub>2</sub> uptake in an Ocean  
636 General Circulation Model. *J. Geophys. Res.* **97**, 3621–3645 (1992).
- 637 39. Matsumoto, K. Radiocarbon-based circulation age of the world oceans. *J. Geophys. Res.* **112**, 1–7  
638 (2007).
- 639 40. Holzer, M. & Primeau, F. W. The path-density distribution of oceanic surface-to-surface transport. *J.*  
640 *Geophys. Res. Ocean.* **113**, 1–22 (2008).
- 641 41. Dong, Y. *et al.* Update on the Temperature Corrections of Global Air-Sea CO<sub>2</sub> Flux Estimates.  
642 *Global Biogeochem. Cycles* **26**, 21–35 (2022).
- 643 42. Matsumoto, K. & Gruber, N. How accurate is the estimation of anthropogenic carbon in the ocean?  
644 An evaluation of the  $\Delta C^*$  method. *Global Biogeochem. Cycles* **19**, (2005).
- 645 43. Bates, N. *et al.* A Time-Series View of Changing Ocean Chemistry Due to Ocean Uptake of  
646 Anthropogenic CO<sub>2</sub> and Ocean Acidification. *Oceanography* **27**, 126–141 (2014).
- 647 44. Gregor, L. & Gruber, N. OceanSODA-ETHZ: a global gridded data set of the surface ocean carbonate  
648 system for seasonal to decadal studies of ocean acidification. *Earth Syst. Sci. Data* **13**, 777–808  
649 (2021).
- 650 45. Broecker, W. S., Takahashi, T., Simpson, H. J. & Peng, T. H. Fate of fossil fuel carbon dioxide and  
651 the global carbon budget. *Science (80-. )*. **206**, 409–418 (1979).
- 652 46. Egleston, E. S., Sabine, C. L. & Morel, F. M. M. Revelle revisited: Buffer factors that quantify the  
653 response of ocean chemistry to changes in DIC and alkalinity. *Global Biogeochem. Cycles* **24**, 1–9  
654 (2010).
- 655 47. Jiang, L. Q., Carter, B. R., Feely, R. A., Lauvset, S. K. & Olsen, A. Surface ocean pH and buffer  
656 capacity: past, present and future. *Sci. Rep.* **9**, 18624 (2019).
- 657 48. Sarmiento, J. L., LeQuéré, C. & Pacala, S. W. Limiting future atmospheric carbon dioxide. *Glob.*  
658 *Biogeochem. Cycles* **9**, 121–137 (1995).
- 659 49. Joos, F. *et al.* An efficient and accurate representation of complex oceanic and biospheric models of  
660 anthropogenic carbon uptake. *Tellus* **48B**, 397–417 (1996).
- 661 50. Keeling, C. D. The Suess Effect: 13-Carbon and 14-Carbon Interactions. in *Environment International*

- 662 2, 229–300 (Pergamon, 1979).
- 663 51. Friedlingstein, P. *et al.* Global Carbon Budget 2020. *Earth Syst. Sci. Data* **12**, 3269–3340 (2020).
- 664 52. Arora, V. K. *et al.* Carbon–concentration and carbon–climate feedbacks in CMIP6 models and their  
665 comparison to CMIP5 models. *Biogeosciences* **17**, 4173–4222 (2020).
- 666 53. Friedlingstein, P. *et al.* Climate-carbon cycle feedback analysis: results from the {C4MIP} model  
667 intercomparison. *J. Clim.* **19**, 3337–3353 (2006).
- 668 54. Meinshausen, M. *et al.* Realization of Paris Agreement pledges may limit warming just below 2 °C.  
669 *Nature* **604**, 304–309 (2022).
- 670 55. Joos, F. *et al.* Carbon dioxide and climate impulse response functions for the computation of  
671 greenhouse gas metrics: A multi-model analysis. *Atmos. Chem. Phys.* **13**, 2793–2825 (2013).
- 672 56. Waugh, D. W., Hall, T. M., Mcneil, B. I., Key, R. & Matear, R. J. Anthropogenic CO<sub>2</sub> in the oceans  
673 estimated using transit time distributions. *Tellus B Chem. Phys. Meteorol.* **58**, 376–389 (2006).
- 674 57. Tanhua, T. *et al.* Ventilation of the Arctic Ocean: Mean ages and inventories of anthropogenic CO<sub>2</sub>  
675 and CFC-11. *J. Geophys. Res.* **114**, 1–11 (2009).
- 676 58. Raimondi, L., Tanhua, T., Azetsu-Scott, K., Yashayaev, I. & Wallace, D. W. R. A 30 -Year Time  
677 Series of Transient Tracer-Based Estimates of Anthropogenic Carbon in the Central Labrador Sea. *J.*  
678 *Geophys. Res. Ocean.* **126**, 1–19 (2021).
- 679 59. Ridge, S. M. & McKinley, G. A. Ocean carbon uptake under aggressive emission mitigation.  
680 *Biogeosciences* **18**, 2711–2725 (2021).
- 681 60. Archer, D., Kheshgi, H. & Maier-Reimer, E. Dynamics of fossil fuel {CO<sub>2</sub>} neutralization by marine  
682 {CaCO<sub>3</sub>}. *Glob. Biogeochem. Cycles* **12**, 259–276 (1998).
- 683 61. Bacastow, R. B. & Keeling, C. D. Models to predict future atmospheric CO<sub>2</sub> concentrations. in  
684 *Workshop on the Global Effects of Carbon Dioxide from Fossil Fuels* (eds. Elliott, W. P. & Machta,  
685 L.) 72–90 (United States Department of Energy, 1979).
- 686 62. Siegenthaler, U. & Oeschger, H. Predicting future atmospheric carbon dioxide levels. *Science* **199**,  
687 388–95 (1978).
- 688 63. Wallace, D. W. R. *Monitoring Global Ocean Carbon Inventories*. (1995).
- 689 64. Gruber, N., Sarmiento, J. L. & Stocker, T. F. An improved method for detecting anthropogenic CO<sub>2</sub>  
690 in the oceans. *Global Biogeochem. Cycles* **10**, 809–837 (1996).
- 691 65. Gruber, N. Anthropogenic CO<sub>2</sub> in the Atlantic Ocean. *Global Biogeochem. Cycles* **12**, 165–191  
692 (1998).
- 693 66. Dickson, A. G., Goyet, C. & DOE. *Handbook of methods for the analysis of the various parameters of*  
694 *the carbon dioxide system in sea water; version 2*. (1994).
- 695 67. Dickson, A. G., Afghan, J. D. & Anderson, G. C. Reference materials for oceanic {CO<sub>2</sub>} analysis: a  
696 method for the certification of total alkalinity. *Mar. Chem.* **80**, 185–197 (2003).
- 697 68. Dickson, A. G. Standards for ocean measurements. *Oceanography* **23**, 34–47 (2010).
- 698 69. Key, R. M. *et al.* A global ocean carbon climatology: Results from Global Data Analysis Project  
699 (GLODAP). *Global Biogeochem. Cycles* **18**, n/a-n/a (2004).
- 700 70. DeVries, T. The oceanic anthropogenic CO<sub>2</sub> sink: Storage, air-sea fluxes, and transports over the  
701 industrial era. *Global Biogeochem. Cycles* **28**, 631–647 (2014).
- 702 71. Orr, J. C. *et al.* Estimates of anthropogenic carbon uptake from four three-dimensional global ocean  
703 models. *Global Biogeochem. Cycles* (2001).
- 704 72. Mikaloff Fletcher, S. E. *et al.* Inverse estimates of anthropogenic CO<sub>2</sub> uptake, transport, and storage  
705 by the ocean. *Global Biogeochem. Cycles* **20**, 1–16 (2006).
- 706 73. Davila, X. *et al.* How Is the Ocean Anthropogenic Carbon Reservoir Filled? *Global Biogeochem.*  
707 *Cycles* **36**, 1–16 (2022).
- 708 74. Groeskamp, S., Lenton, A., Matear, R., Sloyan, B. M. & Langlais, C. Anthropogenic carbon in the  
709 ocean-Surface to interior connections. *Global Biogeochem. Cycles* **30**, 1682–1698 (2016).
- 710 75. Keeling, R. F. & Shertz, S. R. Seasonal and interannual variations in atmospheric oxygen and  
711 implications for the global carbon cycle. *Nature* **358**, 723–727 (1992).
- 712 76. Quay, P. D., Tilbrook, B. & Wong, C. S. Oceanic Uptake of Fossil Fuel CO<sub>2</sub> : Carbon-13 Evidence.

- 713 *Science* (80- ). **256**, 74–79 (1992).
- 714 77. Heimann, M. & Maier-Reimer, E. On the relations between the oceanic uptake of CO<sub>2</sub> and its carbon  
715 isotopes. *Global Biogeochem. Cycles* **10**, 89–110 (1996).
- 716 78. Gruber, N. & Keeling, C. D. An improved estimate of the isotopic air-sea disequilibrium of CO<sub>2</sub> :  
717 Implications for the oceanic uptake of anthropogenic CO<sub>2</sub>. *Geophys. Res. Lett.* **28**, 555–558 (2001).
- 718 79. Khatiwala, S. *et al.* Global ocean storage of anthropogenic carbon. *Biogeosciences* **10**, 2169–2191  
719 (2013).
- 720 80. Friedrich, T. *et al.* Detecting regional anthropogenic trends in ocean acidification against natural  
721 variability. *Nature* **2**, 167–171 (2012).
- 722 81. Munro, D. R. *et al.* Recent evidence for a strengthening CO<sub>2</sub> sink in the Southern Ocean from  
723 carbonate system measurements in the Drake Passage (2002-2015). *Geophys. Res. Lett.* **42**, 7623–  
724 7630 (2015).
- 725 82. Talley, L. D. *et al.* Changes in Ocean Heat, Carbon Content, and Ventilation: A Review of the First  
726 Decade of GO-SHIP Global Repeat Hydrography. *Ann. Rev. Mar. Sci.* **8**, 185–215 (2016).
- 727 83. Wanninkhof, R. *et al.* Detecting anthropogenic CO<sub>2</sub> changes in the interior Atlantic Ocean between  
728 1989 and 2005. *J. Geophys. Res.* **115**, C11028 (2010).
- 729 84. Friis, K., Körtzinger, A., Pätsch, J. & Wallace, D. W. R. On the temporal increase of anthropogenic  
730 CO<sub>2</sub> in the subpolar North Atlantic. *Deep. Res. Part I* **52**, 681–698 (2005).
- 731 85. Goodkin, N. F., Levine, N. M., Doney, S. C. & Wanninkhof, R. Impacts of temporal CO<sub>2</sub> and climate  
732 trends on the detection of ocean anthropogenic CO<sub>2</sub> accumulation. *Global Biogeochem. Cycles* **25**, 1–  
733 11 (2011).
- 734 86. Levine, N. M., Doney, S. C., Wanninkhof, R., Lindsay, K. & Fung, I. Y. Impact of ocean carbon  
735 system variability on the detection of temporal increases in anthropogenic CO<sub>2</sub>. *J. Geophys. Res.* **113**,  
736 C03019 (2008).
- 737 87. Carter, B. R. *et al.* Two decades of Pacific anthropogenic carbon storage and ocean acidification along  
738 Global Ocean Ship-based Hydrographic Investigations Program sections P16 and P02. *Global*  
739 *Biogeochem. Cycles* **31**, 306–327 (2017).
- 740 88. Carter, B. R. *et al.* Pacific Anthropogenic Carbon Between 1991 and 2017. *Global Biogeochem.*  
741 *Cycles* 2018GB006154 (2019). doi:10.1029/2018GB006154
- 742 89. Woosley, R. J., Millero, F. J. & Wanninkhof, R. Rapid anthropogenic changes in CO<sub>2</sub> and pH in the  
743 Atlantic Ocean: 2003-2014. *Global Biogeochem. Cycles* **30**, 70–90 (2016).
- 744 90. Clement, D. & Gruber, N. The eMLR(C\*) Method to Determine Decadal Changes in the Global  
745 Ocean Storage of Anthropogenic CO<sub>2</sub>. *Global Biogeochem. Cycles* **32**, 654–679 (2018).
- 746 91. Tanhua, T., Körtzinger, A., Friis, K., Waugh, D. W. & Wallace, D. W. R. An estimate of  
747 anthropogenic CO<sub>2</sub> inventory from decadal changes in oceanic carbon content. *Proc. Natl. Acad. Sci.*  
748 **104**, 3037–3042 (2007).
- 749 92. Pérez, F. F. *et al.* Atlantic Ocean CO<sub>2</sub> uptake reduced by weakening of the meridional overturning  
750 circulation. *Nat. Geosci.* **6**, 146–152 (2013).
- 751 93. Keeling, C. D. Carbon Dioxide in Surface Ocean Waters: 4. Global Distribution. *J. Geophys. Res.* **73**,  
752 4543–4553 (1968).
- 753 94. Tans, P. P., Fung, I. Y. & Takahashi, T. Observational Constrains on the Global Atmospheric Co<sub>2</sub>  
754 Budget. *Science* (80- ). **247**, 1431–1438 (1990).
- 755 95. Takahashi, T. *et al.* Global air-sea flux of CO<sub>2</sub> : An estimate based on measurements of sea–air pCO<sub>2</sub>  
756 difference. *Proc. Natl. Acad. Sci.* **94**, 8292–8299 (1997).
- 757 96. Takahashi, T. *et al.* Deep-Sea Research II Climatological mean and decadal change in surface ocean  
758 pCO<sub>2</sub> , and net sea – air CO<sub>2</sub> flux over the global oceans. **56**, 554–577 (2009).
- 759 97. Bakker, D. C. E. *et al.* An update to the Surface Ocean CO<sub>2</sub> Atlas (SOCAT version 2). *Earth Syst. Sci.*  
760 *Data* **6**, 69–90 (2014).
- 761 98. Pfeil, B. *et al.* A uniform, quality controlled Surface Ocean CO<sub>2</sub> Atlas (SOCAT). *Earth Syst. Sci.*  
762 *Data* **5**, 125–143 (2013).
- 763 99. Bakker, D. C. E. *et al.* A multi-decade record of high-quality CO<sub>2</sub> data in version 3 of the Surface

- 764 Ocean CO<sub>2</sub> Atlas (SOCAT). *Earth Syst. Sci. Data* **8**, 383–413 (2016).
- 765 100. Rödenbeck, C. *et al.* Data-based estimates of the ocean carbon sink variability - First results of the  
766 Surface Ocean pCO<sub>2</sub> Mapping intercomparison (SOCOM). *Biogeosciences* **12**, 7251–7278 (2015).
- 767 101. Landschützer, P. *et al.* A neural network-based estimate of the seasonal to inter-annual variability of  
768 the Atlantic Ocean carbon sink. *Biogeosciences* **10**, 7793–7815 (2013).
- 769 102. Gregor, L., Lebehot, A. D., Kok, S. & Scheel Monteiro, P. M. A comparative assessment of the  
770 uncertainties of global surface ocean CO<sub>2</sub> estimates using a machine-learning ensemble (CSIR-ML6  
771 version 2019a)-Have we hit the wall? *Geosci. Model Dev.* **12**, 5113–5136 (2019).
- 772 103. Fay, A. R. *et al.* SeaFlux: Harmonization of air-sea CO<sub>2</sub> fluxes from surface pCO<sub>2</sub> data products  
773 using a standardized approach. *Earth Syst. Sci. Data* **13**, 4693–4710 (2021).
- 774 104. Gruber, N. *et al.* Oceanic sources, sinks, and transport of atmospheric CO<sub>2</sub>. *Global Biogeochem.*  
775 *Cycles* **23**, (2009).
- 776 105. Regnier, P., Resplandy, L., Najjar, R. G. & Ciais, P. The land-to-ocean loops of the global carbon  
777 cycle. *Nature* **603**, 401–410 (2022).
- 778 106. Sarmiento, J. L. & Sundquist, E. T. Revised budget for the oceanic uptake of anthropogenic carbon  
779 dioxide. *Nature* **356**, 589–593 (1992).
- 780 107. Regnier, P. *et al.* Anthropogenic perturbation of the carbon fluxes from land to ocean. *Nat. Geosci.* **6**,  
781 597–607 (2013).
- 782 108. Resplandy, L. *et al.* Revision of global carbon fluxes based on a reassessment of oceanic and riverine  
783 carbon transport. *Nat. Geosci.* **11**, (2018).
- 784 109. Landschützer, P., Ilyina, T. & Lovenduski, N. S. Detecting Regional Modes of Variability in  
785 Observation-Based Surface Ocean pCO<sub>2</sub>. *Geophys. Res. Lett.* **46**, 2670–2679 (2019).
- 786 110. Ritter, R. *et al.* Observation-Based Trends of the Southern Ocean Carbon Sink. *Geophys. Res. Lett.*  
787 **44**, 12,339-12,348 (2017).
- 788 111. Gloege, L. *et al.* Quantifying errors in observationally-based estimates of ocean carbon sink  
789 variability. *Global Biogeochem. Cycles* 1–14 (2021). doi:10.1029/2020gb006788
- 790 112. Watson, A. J. *et al.* Revised estimates of ocean-atmosphere CO<sub>2</sub> flux are consistent with ocean carbon  
791 inventory. *Nat. Commun.* **11**, 1–6 (2020).
- 792 113. Wanninkhof, R., Asher, W. E., Ho, D. T., Sweeney, C. & Mcgillis, W. R. Advances in Quantifying  
793 Air-Sea Gas Exchange and Environmental Forcing\*. *Ann. Rev. Mar. Sci.* **1**, 213–244 (2009).
- 794 114. DeVries, T., Holzer, M. & Primeau, F. Recent increase in oceanic carbon uptake driven by weaker  
795 upper-ocean overturning. *Nature* **542**, 215–218 (2017).
- 796 115. Wolter, K. & Timlin, M. S. El Niño/Southern Oscillation behaviour since 1871 as diagnosed in an  
797 extended multivariate ENSO index (MEI.ext). *Int. J. Climatol.* **31**, 1074–1087 (2011).
- 798 116. Frölicher, T. L. *et al.* Dominance of the Southern Ocean in Anthropogenic Carbon and Heat Uptake in  
799 CMIP5 Models. *J. Clim.* **28**, 862–886 (2015).
- 800 117. McKinley, G. A., Rödenbeck, C., Gloor, M., Houweling, S. & Heimann, M. Pacific dominance to  
801 global air-sea {CO<sub>2</sub>} flux variability: A novel atmospheric inversion agrees with ocean models.  
802 *Geophys. Res. Lett.* **31**, (2004).
- 803 118. Lenton, A. & Matear, R. J. Role of the Southern Annular Mode (SAM) in Southern Ocean CO<sub>2</sub>  
804 uptake. *Global Biogeochem. Cycles* **21**, 1–17 (2007).
- 805 119. Keppler, L. & Landschützer, P. Regional Wind Variability Modulates the Southern Ocean Carbon  
806 Sink. *Sci. Rep.* **9**, 7384 (2019).
- 807 120. Le Quéré, C., Takahashi, T., Buitenhuis, E. T., Rödenbeck, C. & Sutherland, S. C. Impact of climate  
808 change and variability on the global oceanic sink of CO<sub>2</sub>. *Global Biogeochem. Cycles* **24**, n/a-n/a  
809 (2010).
- 810 121. Feely, R. A., Wanninkhof, R., Takahashi, T. & Tans, P. Influence of El Niño on the equatorial Pacific  
811 contribution to atmospheric CO<sub>2</sub> accumulation. *Nature* **398**, 597–601 (1999).
- 812 122. Ishii, M. *et al.* Air-sea CO<sub>2</sub> flux in the Pacific Ocean for the period 1990-2009. *Biogeosciences* **11**,  
813 709–734 (2014).
- 814 123. McKinley, G. A., Follows, M. J. & Marshall, J. Mechanisms of air-sea CO<sub>2</sub> flux variability in the

- 815 equatorial Pacific and the North Atlantic. *Global Biogeochem. Cycles* **18**, n/a-n/a (2004).
- 816 124. Chatterjee, A. *et al.* Influence of El Niño on atmospheric CO<sub>2</sub> over the tropical Pacific Ocean:  
817 Findings from NASA’s OCO-2 mission. *Science* (80-. ). **358**, (2017).
- 818 125. Keeling, C. D., Whorf, T. P., Wahlen, M. & v. d. Plicht, J. Interannual extremes in the rate of  
819 atmospheric carbon dioxide since 1980. *Nature* **375**, 666–670 (1995).
- 820 126. Crisp, D. *et al.* How Well Do We Understand the Land-Ocean-Atmosphere Carbon Cycle? *Rev.*  
821 *Geophys.* 1–64 (2022). doi:10.1029/2021rg000736
- 822 127. Angert, A., Biraud, S., Bonfils, C., Buermann, W. & Fung, I. CO<sub>2</sub> seasonality indicates origins of  
823 post-Pinatubo sink. *Geophys. Res. Lett.* **31**, 1999–2002 (2004).
- 824 128. Eddebbar, Y. A. *et al.* El Niño-like physical and biogeochemical ocean response to tropical eruptions.  
825 *J. Clim.* **32**, 2627–2649 (2019).
- 826 129. Marshall, L. R. *et al.* Volcanic effects on climate : recent advances and future avenues. (2022).
- 827 130. Thompson, D. W. J. & Solomon, S. Interpretation of recent Southern Hemisphere climate change.  
828 *Science* **296**, 895–899 (2002).
- 829 131. Hauck, J. *et al.* Seasonally different carbon flux changes in the Southern Ocean in response to the  
830 southern annular mode. *Global Biogeochem. Cycles* **27**, 1236–1245 (2013).
- 831 132. Lovenduski, N. S., Gruber, N. & Doney, S. C. Toward a mechanistic understanding of the decadal  
832 trends in the Southern Ocean carbon sink. *Global Biogeochem. Cycles* **22**, 1–9 (2008).
- 833 133. Gillett, N. P. & Thompson, D. W. J. Simulation of recent southern hemisphere climate change.  
834 *Science* **302**, 273–5 (2003).
- 835 134. Gruber, N., Bates, N. R. & Keeling, C. D. Interannual variability in the Northern Atlantic carbon  
836 sink. *Science* (80-. ). **298**, 2374–2378 (2002).
- 837 135. Frölicher, T. L., Joos, F., Raible, C. C. & Sarmiento, J. L. Atmospheric CO<sub>2</sub> response to volcanic  
838 eruptions: The role of ENSO, season, and variability. *Global Biogeochem. Cycles* **27**, 239–251 (2013).
- 839 136. DeVries, T. Atmospheric CO<sub>2</sub> and Sea Surface Temperature Variability Cannot Explain Recent  
840 Decadal Variability of the Ocean CO<sub>2</sub> Sink. *Geophys. Res. Lett.* **49**, 1–12 (2022).
- 841 137. Terhaar, J., Frölicher, T. L. & Joos, F. Observation-constrained estimates of the global ocean carbon  
842 sink from Earth system models. *Biogeosciences* **19**, 4431–4457 (2022).
- 843 138. Rogelj, J., McCollum, D. L., O’Neill, B. C. & Riahi, K. 2020 emissions levels required to limit  
844 warming to below 2 °C. *Nat. Clim. Chang.* **3**, 405–412 (2012).
- 845 139. Keller, D. P. *et al.* The Effects of Carbon Dioxide Removal on the Carbon Cycle. *Curr. Clim. Chang.*  
846 *Reports* **4**, 250–265 (2018).
- 847 140. Smith, P. *et al.* Biophysical and economic limits to negative CO<sub>2</sub> emissions. *Nat. Clim. Chang.* **6**, 42–  
848 50 (2016).
- 849 141. National Academies of Sciences. *A Research Strategy for Ocean-based Carbon Dioxide Removal and*  
850 *Sequestration*. (National Academies Press, 2022). doi:10.17226/26278
- 851 142. Aricò, S. *et al.* *Integrated Ocean Carbon Research: A Summary of Ocean Carbon Research, and*  
852 *Vision of Coordinated Ocean Carbon Research and Observations for the Next Decade*. (2021).  
853 doi:10.25607/h0gj-pq41
- 854 143. Gruber, N., Boyd, P. W., Frölicher, T. L. & Vogt, M. Biogeochemical extremes and compound events  
855 in the ocean. *Nature* **600**, 395–407 (2021).
- 856 144. Djeutchouang, L. M., Chang, N., Gregor, L., Vichi, M. & Monteiro, P. M. S. The sensitivity of p CO  
857 2 reconstructions to sampling scales across a Southern Ocean sub-domain: a semi-idealized ocean  
858 sampling simulation approach. *Biogeosciences* **19**, 4171–4195 (2022).
- 859 145. Majkut, J. D. *et al.* An observing system simulation for Southern Ocean carbon dioxide uptake.  
860 *Philos. Trans. R. Soc. A Math. Phys. Eng. Sci.* **372**, 20130046–20130046 (2014).
- 861 146. Claustre, H., Johnson, K. S. & Takeshita, Y. Observing the Global Ocean with Biogeochemical-Argo.  
862 *Ann. Rev. Mar. Sci.* **12**, 23–48 (2020).
- 863 147. Gray, A. R. *et al.* Autonomous Biogeochemical Floats Detect Significant Carbon Dioxide Outgassing  
864 in the High-Latitude Southern Ocean. *Geophys. Res. Lett.* **45**, 9049–9057 (2018).
- 865 148. Bushinsky, S. M. *et al.* Reassessing Southern Ocean air-sea CO<sub>2</sub> flux estimates with the addition of

- 866 biogeochemical float observations. *Global Biogeochem. Cycles* **33**, 1–19 (2019).
- 867 149. Verdy, A. & Mazloff, M. R. A data assimilating model for estimating Southern Ocean  
868 biogeochemistry. *J. Geophys. Res. Ocean.* **122**, 6968–6988 (2017).
- 869 150. Carroll, D. *et al.* Attribution of Space-Time Variability in Global-Ocean Dissolved Inorganic Carbon.  
870 *Global Biogeochem. Cycles* **36**, 1–24 (2022).
- 871 151. Bennington, V., Gloege, L. & McKinley, G. A. Variability in the Global Ocean Carbon Sink From  
872 1959 to 2020 by Correcting Models With Observations. *Geophys. Res. Lett.* **49**, (2022).
- 873 152. Lacroix, F., Ilyina, T. & Hartmann, J. Oceanic CO<sub>2</sub> outgassing and biological production hotspots  
874 induced by pre-industrial river loads of nutrients and carbon in a global modeling approach.  
875 *Biogeosciences* **17**, 55–88 (2020).
- 876 153. Kwon, E. Y. *et al.* Stable Carbon Isotopes Suggest Large Terrestrial Carbon Inputs to the Global  
877 Ocean. *Global Biogeochem. Cycles* 1–25 (2021). doi:10.1029/2020gb006684
- 878 154. GESAMP. *High level review of a wide range of proposed marine geoengineering techniques.*  
879 *GESAMP Reports and Studies* (2019).
- 880 155. Dlugokencky, E. & Tans, P. Trends in atmospheric carbon dioxide. *National Oceanic & Atmospheric*  
881 *Administration; Global Monitoring Laboratory (NOAA/GML)* (2022). Available at:  
882 <http://gml.noaa.gov/ccgg/trends/>. (Accessed: 15th July 2015)
- 883 156. Kroeker, K. J. *et al.* Impacts of ocean acidification on marine organisms: quantifying sensitivities and  
884 interaction with warming. *Glob. Chang. Biol.* **19**, 1884–1896 (2013).
- 885 157. Landschützer, P., Gruber, N., Bakker, D. C. E., Stemmler, I. & Six, K. D. Strengthening seasonal  
886 marine CO<sub>2</sub> variations due to increasing atmospheric CO<sub>2</sub>. *Nat. Clim. Chang.* **8**, 146–150 (2018).
- 887 158. Hauck, J. & Völker, C. Rising atmospheric CO<sub>2</sub> leads to large impact of biology on Southern Ocean  
888 CO<sub>2</sub> uptake via changes of the Revelle factor. *Geophys. Res. Lett.* **42**, 1459–1464 (2015).
- 889 159. Gruber, N. & Sarmiento, J. L. Large-scale biogeochemical/physical interactions in elemental cycles.  
890 in *THE SEA: Biological-Physical Interactions in the Oceans* (eds. Robinson, A. R., McCarthy, J. J. &  
891 Rothschild, B. J.) **12**, 337–399 (John Wiley and Sons, 2002).
- 892
- 893
- 894
- 895



**896 Acknowledgements**

897 N.G., J.-D.M., L.G, and P.L. acknowledge support from the European Union’s Horizon 2020 research and  
898 innovation programme under grant agreement. No. 821003 (project 4C). N.G. also acknowledges support  
899 from the E.U. Horizon project no. 821001 (SO-CHIC). The work of D.C.E.B. was supported by the E.U.  
900 Horizon project no. 820989 (COMFORT). The work reflects only the authors’ views; the European  
901 Commission and their executive agency are not responsible for any use that may be made of the information  
902 the work contains. G.A.M. acknowledges funding from NSF through the LEAP STC (2019625) and OCE  
903 (1948624), NASA (80NSSC22K0150) and NOAA (NA20OAR4310340). J.H. received funding from the  
904 Helmholtz Young Investigator Group Marine Carbon and Ecosystem Feedbacks in the Earth System  
905 (MarESys), grant number VH-NG-1301.

906

**907 Author contributions**

908 N.G. led the conceptual design and the implementation and also wrote the first draft. J.-D.M. was responsible  
909 for the generation of Fig 1 and Table 1. P.L. generated Fig 2, L.G. generated Figs 3 and 4, and N.G. drew Fig  
910 5. All authors contributed to the outline, discussed the content and conclusions and provided input to the  
911 manuscript during all drafting stages.

912

**913 Competing interests**

914 The authors declare not competing interests.

915

**916 Peer review information**

917 *Nature Reviews Earth & Environment* thanks [Referee#1 name], [Referee#2 name] and the other,  
918 anonymous, reviewer(s) for their contribution to the peer review of this work.

**919 Publisher's note**

920 Springer Nature remains neutral with regard to jurisdictional claims in published maps and institutional  
921 affiliations.

**922 Supplementary information**

923 Supplementary information is available for this paper at <https://doi.org/10.1038/s415XX-XXX-XXXX-X>

924

925

926  
927 **Tables**  
928  
929  
930  
931

932 TABLE 1.  
 933  
 934 OCEAN CO<sub>2</sub> UPTAKE FROM 1990-2019.  
 935

Method	Reference	Components <sup>(*)</sup>	1990–1999 (Pg C yr <sup>-1</sup> )	2000–2009 (Pg C yr <sup>-1</sup> )	2010–2019 (Pg C yr <sup>-1</sup> )
ATMOSPHERIC CO <sub>2</sub>					
Change in atmospheric CO <sub>2</sub> (ppm)	( <sup>155</sup> )		15.0	18.7	23.6
OCEAN CO <sub>2</sub> UPTAKE					
Change in interior accumulation of ant. CO <sub>2</sub> (†)	( <sup>4</sup> )	F <sub>ant</sub> <sup>ss</sup> + F <sub>ant</sub> <sup>ns</sup>	-2.1±0.2	-2.6±0.3	-3.3±0.3
Ocean inverse model (Green’s function)	( <sup>3</sup> )	F <sub>ant</sub> <sup>ss</sup>	-2.0±0.6	-2.3±0.6	NA
Ocean inverse model (Adjoint)	( <sup>136</sup> )	F <sub>ant</sub> <sup>ss</sup>	-2.2±0.1	-2.5±0.1	-2.9±0.2
Ocean inverse model (Adjoint) (§)	( <sup>136</sup> )	F <sub>ant</sub> <sup>ss</sup> + F <sub>nat</sub> <sup>ns</sup>	-2.0±0.1	-2.3±0.1	-2.7±0.2
Ocean forward models	( <sup>25</sup> )	F <sub>ant</sub> <sup>ss</sup> + F <sub>ant</sub> <sup>ns</sup> + F <sub>nat</sub> <sup>ns</sup>	-2.0±0.2	-2.1±0.3	-2.5±0.3
Surface ocean pCO <sub>2</sub> products (#)	( <sup>103</sup> )	F <sub>ant</sub> <sup>ss</sup> + F <sub>ant</sub> <sup>ns</sup> + F <sub>nat</sub> <sup>ns</sup>	-2.1±0.4	-2.3±0.2	-3.1±0.2

936  
 937 (\*) F<sub>ant</sub><sup>ss</sup> : steady-state uptake flux component of anthropogenic CO<sub>2</sub> (part driven solely by the increase in atmospheric  
 938 CO<sub>2</sub>); F<sub>ant</sub><sup>ns</sup>: non-steady-state uptake component of anthropogenic CO<sub>2</sub> (part driven by variations in ocean circulation and  
 939 other physical drivers); F<sub>nat</sub><sup>ns</sup>: non-steady-state exchange component of natural CO<sub>2</sub> (part driven by variations in ocean  
 940 circulation and other physical drivers). (see Box 1)  
 941 (†) scaled using β = 1.39 Pg C/ppm CO<sub>2</sub> and the change in atmospheric pCO<sub>2</sub> indicated in the first line.  
 942 (§) Non-steady component is only due to SST variability (warming).  
 943 (#) Adjusted for the steady-state outgassing of river derived CO<sub>2</sub>.  
 944

945  
946  
947  
948  
949  
950  
951  
952  
953  
954  
955  
956  
957  
958  
959  
960  
961  
962  
963  
964  
965  
966  
967  
968  
969  
970  
971  
972  
973  
974  
975  
976

## Box 1 | Key concepts in ocean carbon sink investigations

### [bH1] Natural versus anthropogenic CO<sub>2</sub>

A key concept aiding the interpretation of the ocean carbon sink has been the separation of the air-sea CO<sub>2</sub> fluxes and the changes in the ocean interior storage of DIC into natural and anthropogenic CO<sub>2</sub> components<sup>38</sup>.

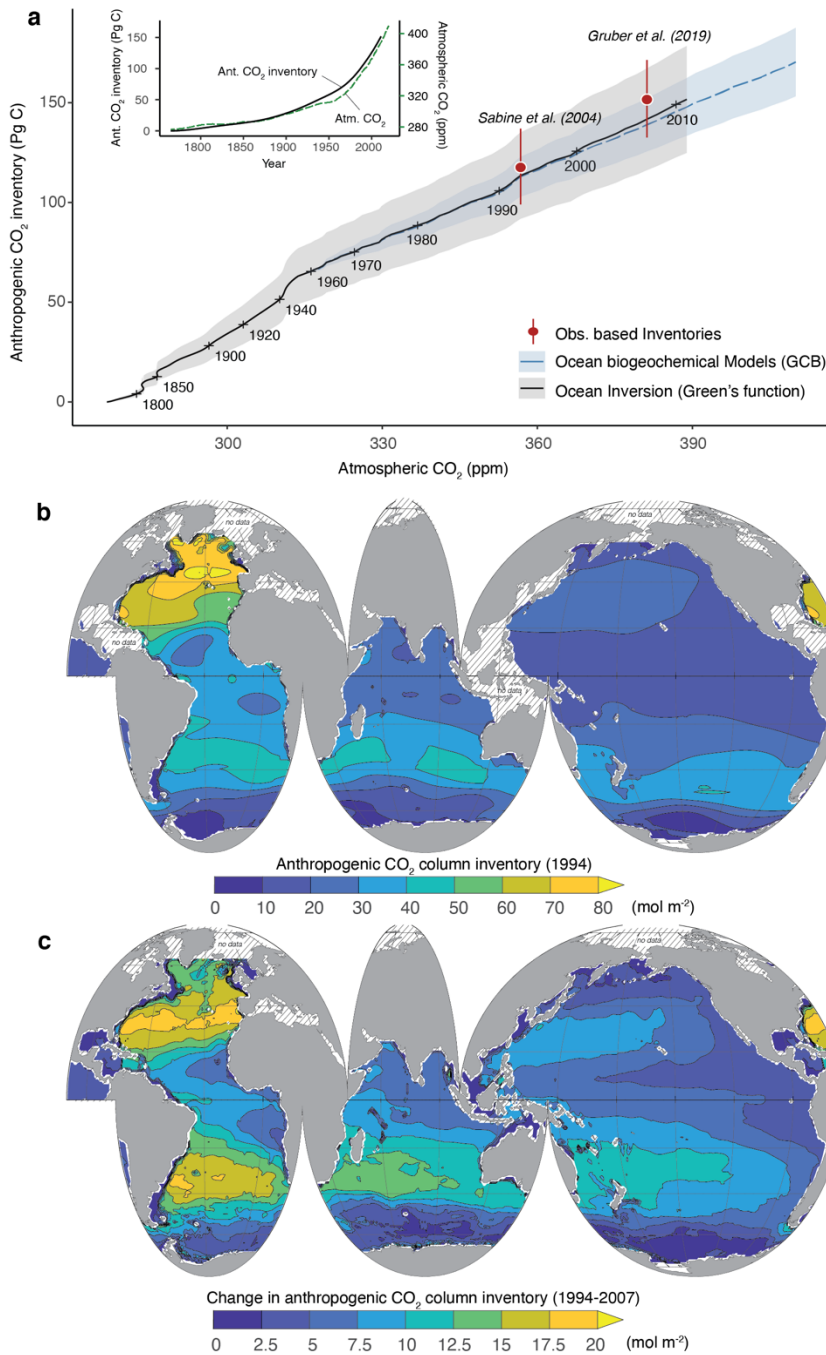
The natural CO<sub>2</sub> component ( $C_{\text{nat}}$ ) is the part of the ocean's DIC pool that existed in pre-industrial times. This pool is involved in many processes, namely air-sea gas exchange, uptake and release by the biological pumps, interactions with and loss to the sediments, and input by rivers (Box Figure 1a). The anthropogenic component ( $C_{\text{ant}}$ ) represents the perturbation to the DIC pool, driven by the anthropogenically-driven increases in atmospheric CO<sub>2</sub>. It is substantially smaller than the natural DIC pool (Box Figure 1b).

An important assumption that has simplified analysis is that the anthropogenic CO<sub>2</sub> component does not interact with the natural CO<sub>2</sub> component<sup>38</sup>. Therefore, the only processes of importance for anthropogenic CO<sub>2</sub> are the uptake from the atmosphere via air-sea gas exchange and the subsequent transport to depth (Box Figure 1a). The assumption about the lack of interaction between the two pools is generally well met, but there are some exceptions. For example, the acidification induced by the oceanic accumulation of anthropogenic CO<sub>2</sub> can affect ocean biology<sup>156</sup> and also has been shown to modify the flux of natural CO<sub>2</sub><sup>157,158</sup>.

### [bH1] The steady state ocean

The second key concept is steady-state, which is reached if climate forcing remains constant for long enough for ocean circulation and ocean biology to become unchanging with time. In this situation, natural CO<sub>2</sub> fluxes across the air-sea interface balance to zero on a global scale<sup>104</sup>, with the exception of steady-state outgassing of river-derived CO<sub>2</sub><sup>105</sup>. Biological fluxes are also balanced over the annual cycle. The only variations in time come from the steady-state uptake of anthropogenic CO<sub>2</sub> (Box Figure 1c, e). If climate is permitted to vary, leading to a non-steady-state situation, both natural and anthropogenic CO<sub>2</sub> components are affected, leading to additional fluxes and changes in storage (Box Figure 1 d,f). The non-steady-state component of natural CO<sub>2</sub> emerges from a situation where climate is varying, but where atmospheric CO<sub>2</sub> is kept at its preindustrial level. The difference between this situation with one where atmospheric CO<sub>2</sub> is permitted to increase gives the non-steady-state component of anthropogenic CO<sub>2</sub> (Box Figure 1, c-f).

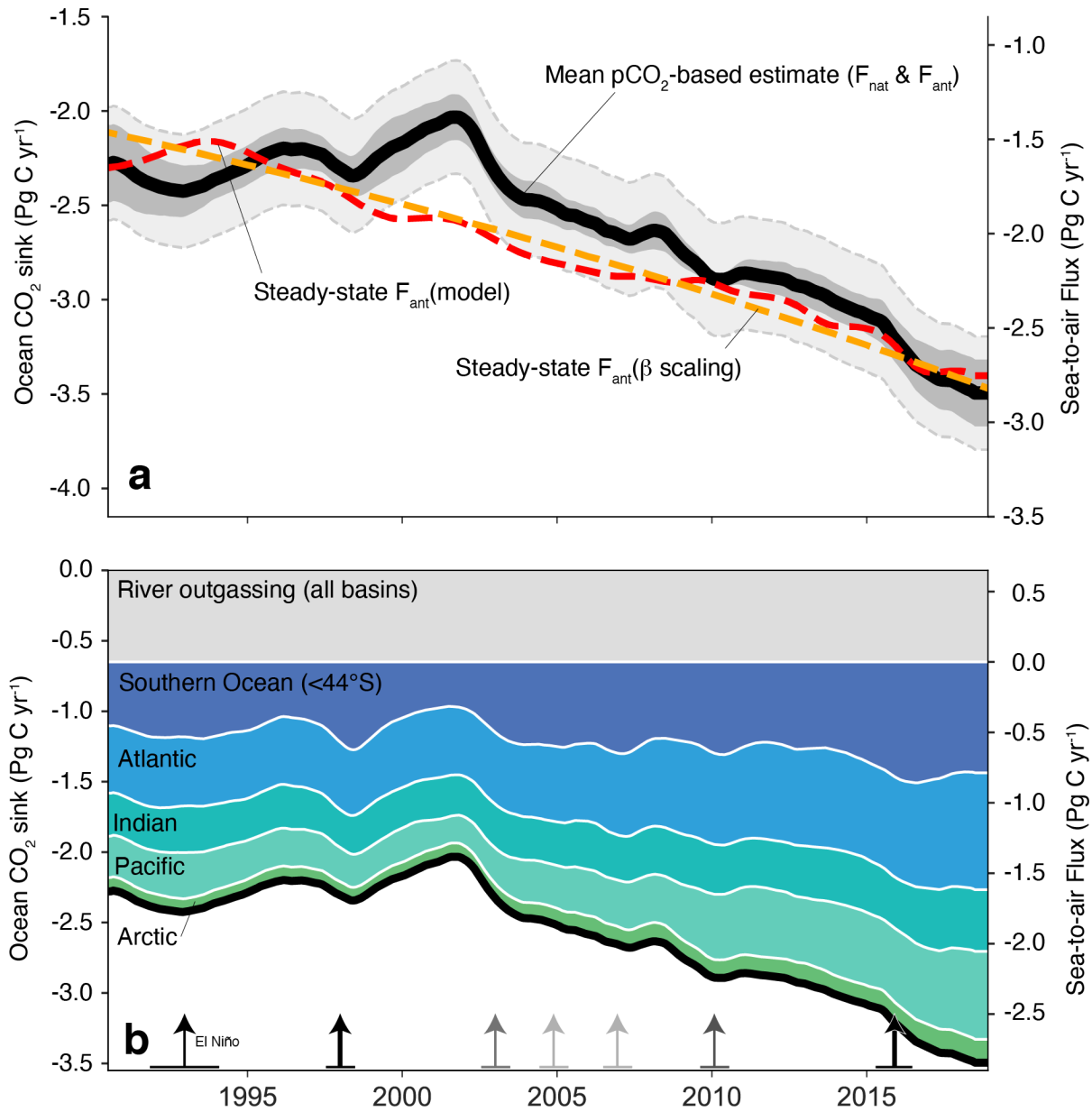
977 **Figures**



978  
 979 **Fig 1. Ocean uptake and storage of anthropogenic CO<sub>2</sub>.** a | Temporal progression of the total ocean  
 980 inventory of anthropogenic CO<sub>2</sub> as a function of the atmospheric CO<sub>2</sub> content. Results are from an ocean  
 981 inverse model<sup>3</sup> (black line and grey shaded band indicating uncertainty) spanning the period from 1765 until  
 982 2010, the ocean biogeochemical model results used in the Global Carbon Budget<sup>25</sup> (blue line for the mean  
 983 and blue shaded band representing the standard deviation), and two observation based estimates of the ocean  
 984 interior accumulation of anthropogenic CO<sub>2</sub><sup>2,4</sup> for 1994 and 2007. The inset shows the time history of  
 985 atmospheric CO<sub>2</sub> and the ocean CO<sub>2</sub> uptake<sup>3</sup>. The bands represent the cumulative uncertainty from the start of  
 986 the respective estimate. The nearly linear scaling of the ocean uptake with the atmospheric CO<sub>2</sub> content is

987 particularly evident after 1959. The ocean biogeochemical model results shown here include also the non-  
988 steady-state, component of natural CO<sub>2</sub> (climate variability). **b** | Column inventory of anthropogenic CO<sub>2</sub> in  
989 mol m<sup>-2</sup> for the year 1994 estimated using the ΔC\* back-calculation method <sup>2</sup>. Strong regional patterning of  
990 the accumulation of anthropogenic CO<sub>2</sub> in the ocean was driven by regional differences in ocean circulation  
991 and mixing. **c** | Change in the water column inventory between 1994 and 2007 estimated by the eMLR(C\*)  
992 method <sup>4</sup>. In b and c, the hatching indicates regions that were not mapped.  
993

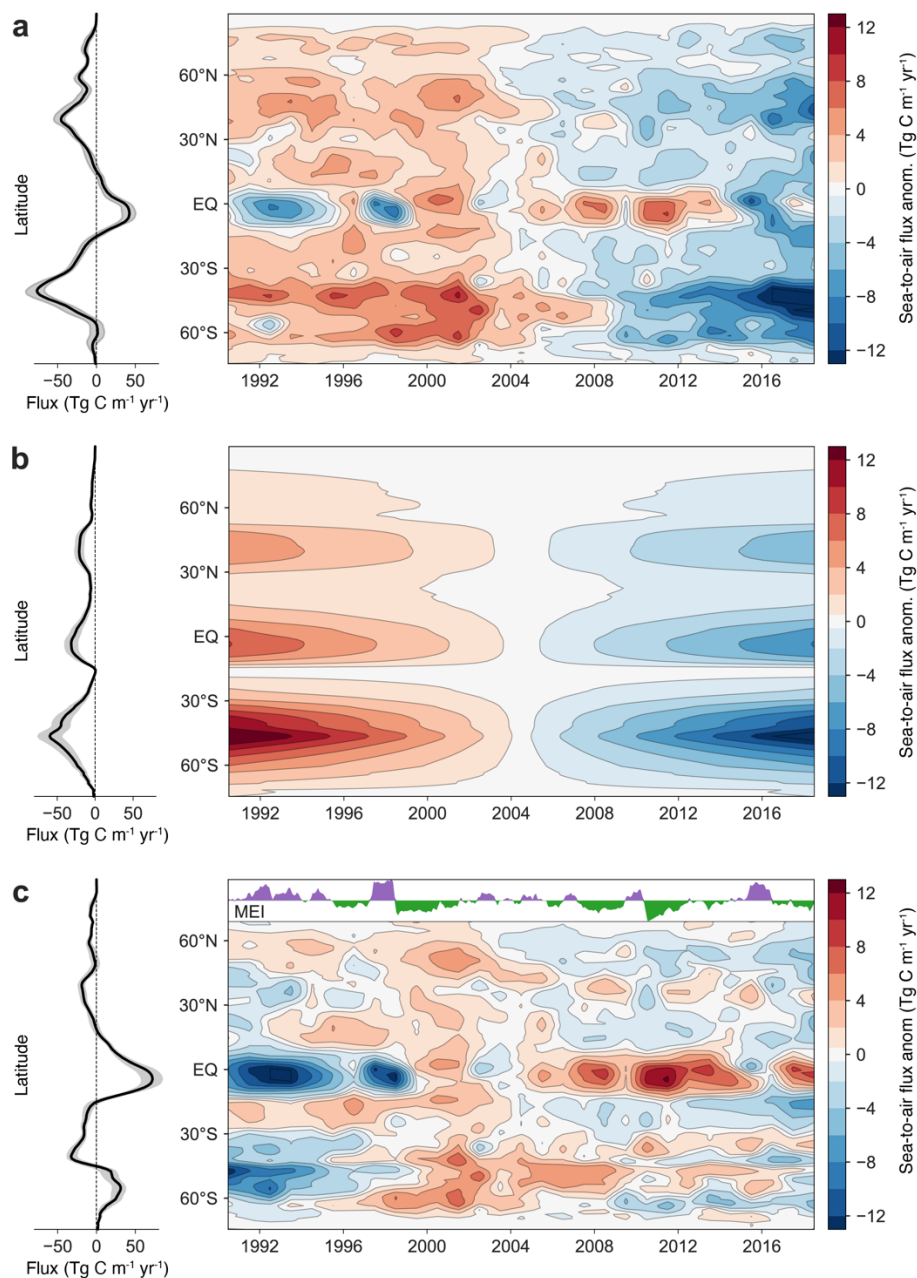




1005  
 1006  
 1007 **Fig 3. Temporal evolution of the global ocean CO<sub>2</sub> sink a** | Global ocean CO<sub>2</sub> sink estimated by the 6 pCO<sub>2</sub>  
 1008 observation based products contained in SeaFlux<sup>103</sup>. The estimated net sea-to-air fluxes were adjusted by the  
 1009 steady-state river outgassing flux of 0.65 Pg C yr<sup>-1</sup><sup>105</sup> to obtain the ocean CO<sub>2</sub> sink flux that is of relevance  
 1010 for balancing the global sources and sinks of CO<sub>2</sub> (the natural flux, F<sub>nat</sub>, plus the anthropogenic flux, F<sub>ant</sub>). The  
 1011 solid black line indicates the mean estimate with the dark grey area representing the standard error across the  
 1012 6 products. The dashed grey lines indicate the uncertainty of the ocean sink and include the uncertainty of  
 1013 ±0.30 Pg C yr<sup>-1</sup> associated with the river outgassing flux<sup>105</sup>. The dashed red line represents the steady-state  
 1014 uptake of anthropogenic CO<sub>2</sub> estimated from a global ocean model (CESM-ETHZ<sup>25</sup>). The dashed orange line  
 1015 represents the expected steady-state uptake of anthropogenic CO<sub>2</sub> estimated from the sensitivity β (left axis).  
 1016 **b** | Contribution of individual ocean basins (north of 44°S) to the global ocean CO<sub>2</sub> sink based on the  
 1017 ensemble mean of the SeaFlux products. The grey band represents the steady-state oceanic outgassing of  
 1018 river-derived CO<sub>2</sub>. It was not allocated to individual basins. El Niño related variations in the Pacific basin are



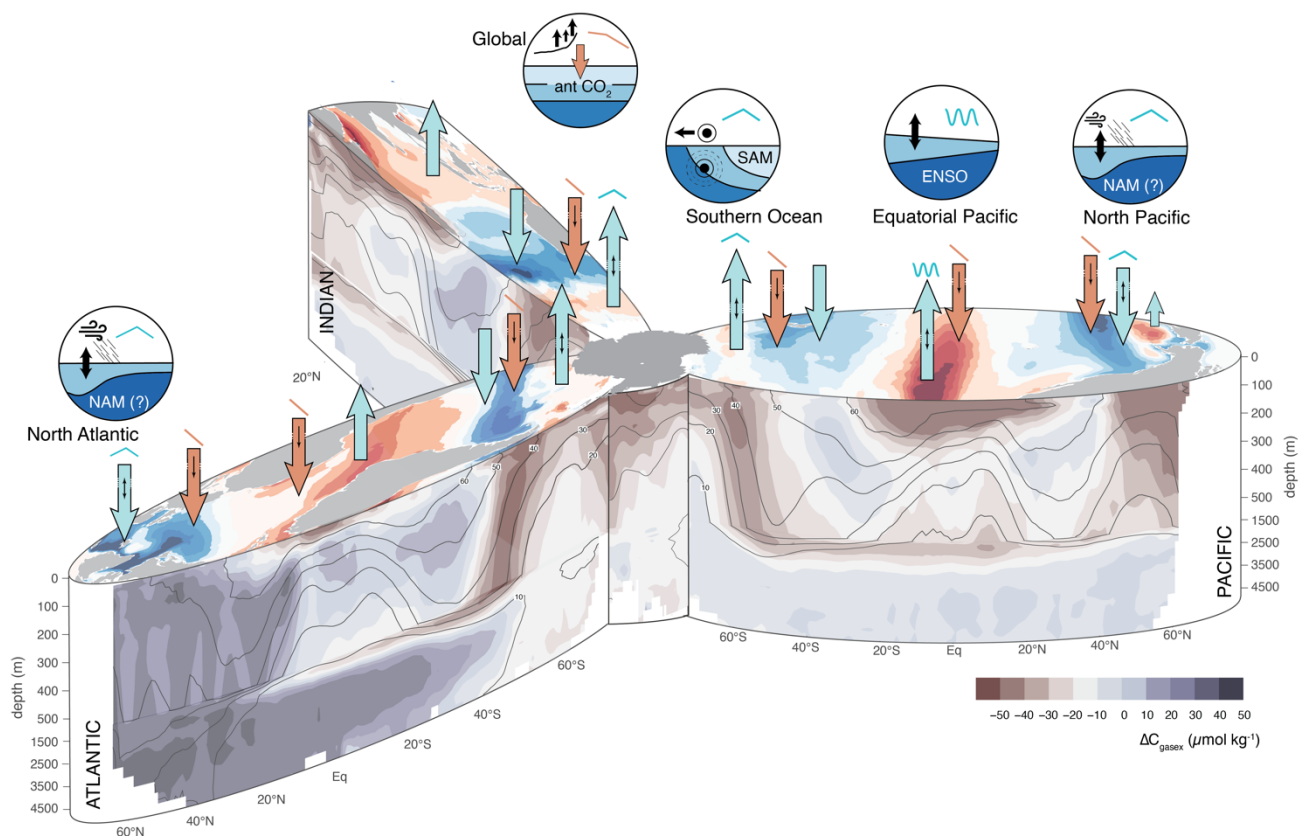
1019 represented by arrows, with the grey shading indicating strength (darker arrows for stronger events).The  
1020 global ocean carbon sink varies substantially in time around the long-term trend given by the steady-state  
1021 uptake of anthropogenic CO<sub>2</sub> with a period of stagnant uptake in the 1990s followed by a period of faster than  
1022 expected growth of the ocean carbon sink after the turn of the millennium.  
1023



1024  
1025  
1026  
1027  
1028  
1029  
1030  
1031  
1032  
1033  
1034  
1035  
1036

**Fig 4. Zonally integrated anomalous CO<sub>2</sub> fluxes and its components. a** | Hovmoeller diagram of the annual mean, zonal mean anomalies of the total air-sea CO<sub>2</sub> fluxes as a function of time and latitude (right panels) together with the zonal mean (left panels). The anomalies were computed by subtracting the long-term mean flux from the annual mean flux for a given year using the ensemble mean data from the SeaFlux product<sup>103</sup>. The ribbon in the left panels shows the range of the integrated fluxes relative to the zonal mean. The zonal mean dominates compared to the interannual variability. **b** | The same as a, but for the anomalous air-sea fluxes of the steady-state component of anthropogenic CO<sub>2</sub>. This estimate was obtained by scaling the ocean inversion-based estimate<sup>72</sup> for 1995 with a  $\beta$  of  $1.4 \text{ Pg C (ppm CO}_2\text{)}^{-1}$ . The anomalies were then obtained by subtracting the long-term mean flux. **c** | The same as a, but for the anomalous air-sea fluxes of the non-steady-state component of CO<sub>2</sub>, obtained by subtracting b from a. There is strong interannual variability of the air-sea fluxes in the tropics, largely associated with El Niño/Southern Oscillation (ENSO) dynamics as

1037 indicated by the timeseries of the multivariate ENSO index (MEI)<sup>115</sup> in panel c, and the strong decadal  
1038 variations in the Southern Ocean, largely driven by the non-steady state components.  
1039



1040  
 1041  
 1042  
 1043  
 1044  
 1045  
 1046  
 1047  
 1048  
 1049  
 1050  
 1051  
 1052  
 1053  
 1054  
 1055  
 1056

Fig 5. **Interannual to decadal variability in the ocean carbon sink.** The global ocean sources and sinks of CO<sub>2</sub> are shown along the surface ocean. The ocean interior distribution of the gas-exchange component of natural CO<sub>2</sub><sup>104,159</sup> (colors) and of the total amount of anthropogenic CO<sub>2</sub> for 2007<sup>2,4</sup> (isolines) are shown along the depth profile. The hotspots for interannual and decadal variability are noted by the insets. Gradients in the gas-exchange component of natural CO<sub>2</sub> reflects the addition or removal of natural CO<sub>2</sub> through air-sea exchange at the surface. The turquoise arrows indicate the sea-to-air fluxes of natural CO<sub>2</sub> including the type and direction of variability (hat: decadal variability, waves: interannual variability). The reddish arrows indicate the oceanic uptake of anthropogenic CO<sub>2</sub> which is increasing everywhere (straight line). Not shown as arrows is the outgassing flux of the river-derived natural CO<sub>2</sub>. The icons relate the variations in the dominant regions of variability (tropical Pacific, and the higher latitudes) to the underlying processes, such as El Niño-Southern Oscillation (ENSO) in the tropical Pacific, and the high latitude modes of variability, especially the Southern Annular Mode (SAM) and the Northern Annular Mode (NAM). Changes in atmospheric CO<sub>2</sub> growth rates affect the global uptake of anthropogenic CO<sub>2</sub>.

1057  
 1058  
 1059  
 1060  
 1061  
 1062  
 1063  
 1064  
 1065  
 1066  
 1067  
 1068  
 1069  
 1070  
 1071  
 1072  
 1073  
 1074  
 1075  
 1076  
 1077  
 1078  
 1079  
 1080  
 1081  
 1082  
 1083  
 1084  
 1085  
 1086  
 1087  
 1088  
 1089  
 1090  
 1091  
 1092  
 1093  
 1094  
 1095  
 1096  
 1097  
 1098  
 1099  
 1100  
 1101

**Glossary**

**AIR-SEA GAS EXCHANGE**

A diffusion-driven process governing the transfer of gases across the air-sea interface, driven by the concentration gradient of the gas across the interface and controlled by the level of turbulence at the interface.

**BUFFER FACTOR (REVELLE FACTOR)**

The ocean’s buffer factor describes how well seawater is able to buffer an increase in surface ocean CO<sub>2</sub> (pCO<sub>2</sub>) and is thus crucial for determining the amount of anthropogenic CO<sub>2</sub> the surface ocean can hold.

**CARBON, DISSOLVED INORGANIC (DIC)**

Dissolved inorganic carbon (DIC) is the sum of all dissolved inorganic carbon species in the seawater, and includes dissolved CO<sub>2</sub> (CO<sub>2</sub><sup>aq</sup>), carbonic acid (H<sub>2</sub>CO<sub>3</sub>), bicarbonate (HCO<sub>3</sub><sup>-</sup>), and carbonate (CO<sub>3</sub><sup>2-</sup>).

**CO<sub>2</sub>, OCEANIC PARTIAL PRESSURE OF (pCO<sub>2</sub>)**

The oceanic partial pressure of CO<sub>2</sub>, pCO<sub>2</sub><sup>oc</sup> or often just pCO<sub>2</sub>, is the partial pressure of CO<sub>2</sub> measured in the air in equilibrium with the water parcel under consideration at one atmosphere total pressure and at the in-situ temperature of the water parcel.

**EL NIÑO - SOUTHERN OSCILLATION (ENSO)**

The El Niño-Southern Oscillation is a quasi-periodic oscillation of the coupled ocean-atmosphere system with the majority of the action being focused on the eastern tropical Pacific; it is globally the dominant mode of climate variability.

**INVERSE MODELS**

Inverse models describe a class of models that fuse observations and models in order to improve our quantitative understanding of a set of processes.

**FORCING, INTERNAL AND EXTERNAL**

Processes leading to changes in the ocean carbon sink: Internal forcing is primarily associated with (internally generated) weather and climate variations, while external forcing is driven by processes external to the climate system, such as volcanic eruptions.

**FORWARD MODELS**

Forward models, such as those used for the Global Carbon Budget, are a class models that start from initial conditions and solve the governing balance equations by time-integrating them forward using a set of provided boundary conditions.

**OCEAN ACIDIFICATION**

Change in the ocean’s seawater chemistry (pH, [CO<sub>3</sub><sup>2-</sup>], CaCO<sub>3</sub> saturation state, etc) as a consequence of the oceanic uptake of anthropogenic CO<sub>2</sub>.

1102

1103 OCEAN BIOGEOCHEMICAL MODELS

1104 Ocean biogeochemical models are a class of ocean models where the most important biogeochemical  
1105 processes are explicitly represented, namely air-sea gas exchange, chemical speciation, and biological  
1106 processes.